NBSIR 85-3107

Field Performance of Three Residential Heat Pumps in the Cooling Mode

Walter H. Parken
David A. Didion
Paul H. Wojciechowski
Lih Chern

U.S. DEPARTMENT OF COMMERCE
National Bureau of Standards
Center for Building Technology
Building Equipment Division
Gaithersburg, Maryland 20899

March 1985

Sponsored By:

U.S. Department of Energy
Office of Building Energy Research and Development
Washington, D.C. 20585

NBSIR 85-3107

FIELD PERFORMANCE OF THREE RESIDENTIAL HEAT PUMPS IN THE COOLING MODE

Walter H. Parken
David A. Didion
Paul H. Wojciechowski
Lih Chern

U.S. DEPARTMENT OF COMMERCE
National Bureau of Standards
Center for Building Technology
Building Equipment Division
Gaithersburg, Maryland 20899

March 1985

Sponsored By:

U.S. Department of Energy
Office of Building Energy Research
and Development
Washington, D.C. 20585

U.S. DEPARTMENT OF COMMERCE, Malcolm Baldrige, *Secretary*
NATIONAL BUREAU OF STANDARDS, Ernest Ambler, *Director*

ABSTRACT

This report presents the results of a field performance study of heat pumps operating in the cooling mode. The objective of this study was to develop a method for calculating seasonal field performance parameters as well as to compare field performance and laboratory results. This comparison is necessary to determine how well the testing and rating standards required of heat pump and standard central air conditioning manufacturers predict actual field performance. It was determined that the laboratory test procedures were too high with respect to cycling rate and that a somewhat lower rate should be employed. Field thermostat data was also collected and used to develop a semi-empirical model.

Key Words: Central air conditioners; cooling seasonal performance; field performance; field performance of heat pumps; heat pumps; heat pump test methods; modelling; thermostat

ACKNOWLEDGEMENTS

This study was sponsored by the U.S. Department of Energy, Office of Building Energy Research and Development.

TABLE OF CONTENTS

LIST OF TABLES

LIST OF FIGURES

NOMENCLATURE

c - time (minutes) after unit cycles on for condensate to form on coil

C_D - degradation coefficient

CLF - cooling load factor

EER - energy efficiency ratio

N - cycling rate (cycles/h)

N_{max} - cycling rate at 50 percent on-time

PLF - part-load factor, $PLF = EER_{cyc}/EER_{ss}$

p, q - constants in the equation $PLF = 1 - e^{-p(CLF)^q}$

Q - cooling done

$\dot{Q}$ - capacity

t_{on} - length of on-time in one cycle

t_{off} - length of off-time in one cycle

T_j - outdoor temperature, bin (T_{out}(°F))

W - energy input

$\dot{W}$ - power input

Γ - fractional on-time, t_{on}/τ

Γ_i - fractional on-time bin

τ - total time period for a complete on-off cycle

Subscripts

ss - steady-state

cyc - cyclic

seas - seasonal

i - fractional on-time bin number

j - outdoor temperature bin number

k - a single on-off cycle

Superscripts

ℓ - latent

s - sensible

t - total

SI CONVERSION FACTORS

MULTIPLY	BY	TO OBTAIN
Btu/h, Btuh	0.293	W
Btu/lbm°F, [C_p, specific heat]	4.19	kJ/kg°C
°F	°C = (°F - 32)/1.8	
ft	0.3048	m
ft/min, fpm	0.00508	m/s
ft^3/lbm	0.0623	m^3/kg
ft^3/min, CFM	0.472	m^3/s
gpm (US)	0.0631	L/S
inch	25.4	mm
inch of water	3.38	kPa
kBtu/h	1055	kJ
lbm/h	0.126	g/s
ton of refrigeration capacity	3516	W

1. INTRODUCTION

Methods of laboratory testing, rating and estimating the heating and cooling seasonal performance of heat pumps have been established in research previously performed and documented at the National Bureau of Standards (NBS) [1,2]. This research became the basis for the development of test procedures for central air conditioners and heat pumps issued by the United States Department of Energy in December 1979 [3]. In order to further verify and refine the test procedures, reliable data from field installed heat pumps were required in order to correlate their performance with independent laboratory tests. To accomplish this, NBS began monitoring, in June 1980, the field performance of three residential heat pumps located in the Washington, D.C. area. A microprocessor-based data acquisition system, located at each site, was used to gather, reduce, and analyze data during the cooling and heating seasons of 1980 and 1981. A previous report describes the development of the monitoring procedures, instrumentation, and microprocessor-related hardware and software used in the heat pump performance monitoring and evaluation [4].

This report presents the cooling performance results of three field-located residential heat pumps for the 1980 cooling season. This program required the examination, reduction and analysis of large amounts of data and this report represents the summary of the results. The objectives of the cooling portion of the field investigation were to:

(1) Provide manufacturers, modelers, government agencies and others with accurate, complete and realistic field performance data;

(2) Present field thermostat data and develop a thermostat model to predict cycling times;

(3) From the field performance data, develop a method for calculating the seasonal field performance parameters;

(4) Present laboratory results for the steady-state and cyclic cooling performance of a similar central air conditioner or heat pump model as used in the field study;

(5) Compare field performance and laboratory results to determine how well the testing and rating standards (Ref. 3) required of heat pump and central air conditioning manufacturers predict actual field performance; and

(6) Evaluate and critically review the types of data and data acquisition requirements needed for accurate and complete evaluation for the field testing of heat pumps and central air conditioners.

2. SELECTION AND DESCRIPTION OF FIELD UNITS

The heat pumps monitored in this field study were units already operating in residences of NBS employees who volunteered to participate in the program. The heat pumps to be evaluated were selected on the basis of a number of criteria, including the following: (1) the unit had to be an air-source heat pump model available for procurement for additional laboratory testing; (2) the unit must have been installed and operating in a manner recommended by the manufacturer; (3) the unit had to be the only system providing heating and cooling within the residence; (4) ductwork had to have straight sections long enough for the proper installation of air flowrate and temperature sensing devices; and (5) all dwellings had to be located close enough to NBS in Gaithersburg, Maryland to permit frequent monitoring and to minimize travel time and associated costs.

Three split system air-to-air heat pumps were eventually selected and instrumented for the study. A brief description of the three installations is given below:

Unit number one was a 2 1/2 ton, air-source, unitary heat pump. In the cooling mode the unit utilized a non-bleed refrigerant thermal expansion valve. Along with the indoor coil, the air handler contained 15 kW of auxiliary heater elements. All ductwork (both return and supply) was insulated on the inside. It was installed in a one-story, ranch-style residence with brick exterior. A large part of the basement was used for living quarters, with a total conditioned floor area of approximately 2900 ft^2. The house was situated on an open, level plane and not shaded by trees or other structures. Throughout the test period, the house was vacant during working hours (occupied on weekends during the day).

Unit number two, a 3 ton unitary, air-source heat pump, also contained 15 kW of auxiliary electric resistance heaters located in the indoor section. The unit utilized a constant area refrigerant expansion device. Return ductwork was insulated on the inside while the supply ductwork had insulation on the outside. The unit was installed in a one-story, wood frame structure with approximately 1800 ft^2 of living space including a basement family room. The house was situated near many large trees, but received direct sunlight from the south and west. The exterior was

painted a dark color. During the test period, the house was usually occupied by two or more people throughout the day.

Unit number three also contained 15 kW of auxiliary electric resistance heaters located in the indoor section and employed a constant area refrigerant expansion device. This unit, like unit number two, was a 3 ton air-source, unitary heat pump. Ductwork was not insulated. The unit was installed in a 1 1/2 story, wood frame house which had a light beige exterior. The house was not shaded by trees or other structures. Total living area is approximately 1600 ft^2. The basement (another 1000 ft^2) was not used as a regular living quarters. During the test period the house was unoccupied during normal working hours on weekdays.

3. FIELD DATA ACQUISITION SYSTEM

3.1 System Description

The field instrumentation data acquisition system is described in a previous report, NBSIR 81-2285, (Ref. 4). An on-line microcomputer at each field site performed the following functions: (1) control of the data monitoring strategy; (2) processing of data obtained from the analog and digital instrumentation to engineering units; (3) performing computational analysis; and (4) recording the results on magnetic (floppy) disks. Field-located disks were replaced every seven to ten days, at which time manual checks on field unit operation and periodic instrument calibrations were made. A central microcomputer located at NBS was used to further process the data contained on disks recorded in the field. This central computer was a Z-80 based computer with two 5 1/4 inch floppy disks and 64K of static RAM memory. Peripherals included a CRT monitor and a printer.

3.2 Measurements and Instrumentations

Measurements of fourteen heat pump related functions--twelve analog and digital inputs plus two on/off mode conditions--were made and recorded at each field location. A schematic illustration of the nature and location of each measurement is given in figure 3.1.

Outdoor ambient dry bulb temperature was monitored and recorded for the 1980 cooling season using a calibrated linearized-thermister sensor located in a 'bird house'--a vented wooden box mounted directly on the north-facing exterior wall of the residence. Table 3.1 summarizes quantities which were measured and the type of sensing element used for each measurement. A

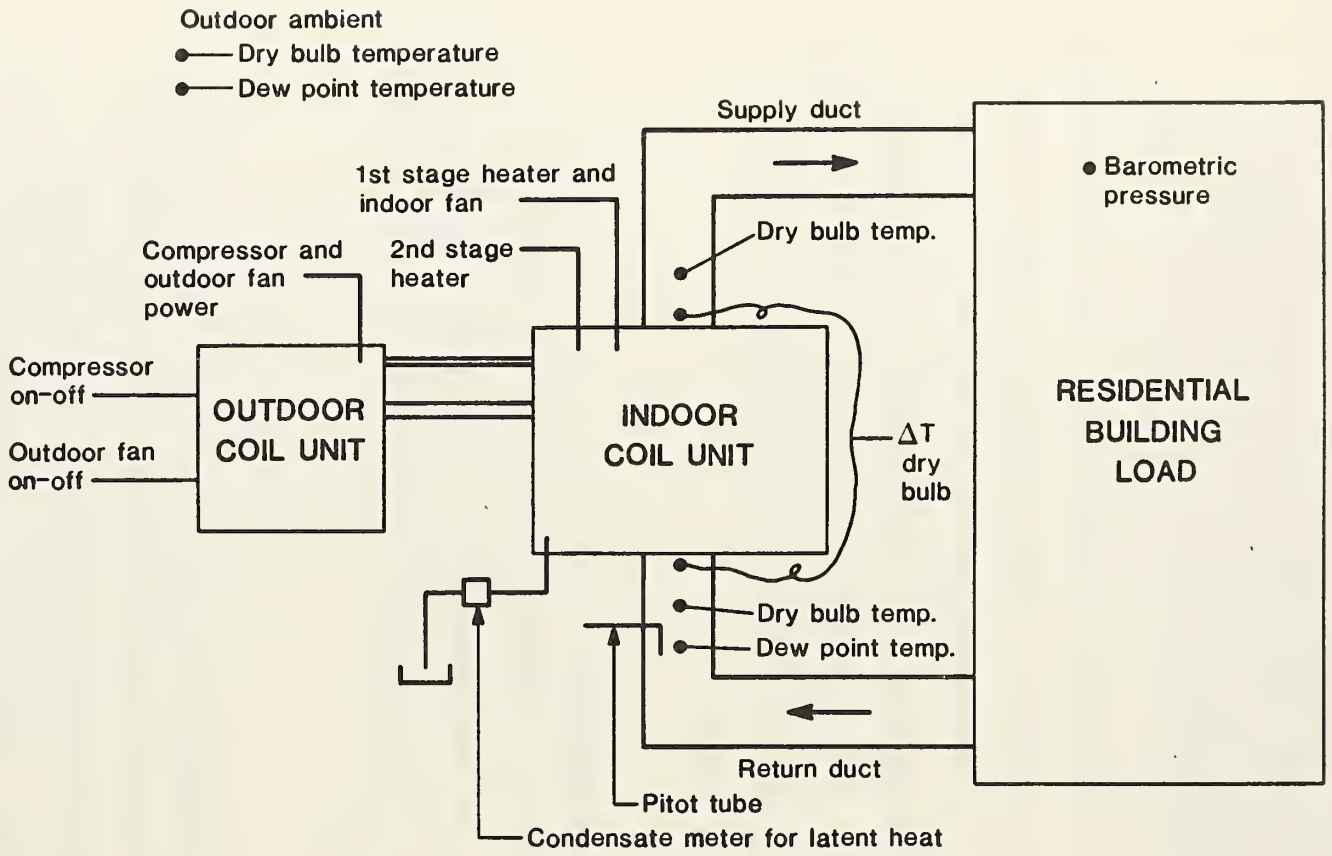

Figure 3.1. Schematic of instrumentation for typical field unit showing location of 12 sensing elements.

Table 3.1 Description of Data Recorded in Field Tests

	Measured Quantity and Units	Symbol	Sensing Element (or Calculated)	Data Acquisition [1] Scan	Cyclic	Daily	Half Hour
1	Pitot tube differential pressure (inches H_2O)	DP	Pitot tube with variable capacitance ΔP cell	IV[2]			
2	Return air dew point temp. (F)	TDPR	LiCℓ/RTD dew point cell	IV	CTIA	CTIA	IV
3	Outdoor air dew point temp. (F)	TDPO	LiCℓ/RTD dew point cell	IV		HSA	
4	Barometric pressure (inches H_2O)	PATM	Pressure cell with diaphragm potentiometer	IV			IV
5	Return air dry bulb temp. (F)	TRET	Linear thermistor	IV	CTIA	CTIA	IV
6	Outdoor air dry bulb temp. (F)	TOUT	Linear thermistor	IV	EOC	HSA	IV
7	Differential temp. across indoor coil	DT	Type-T thermocouple	IV			IV
8	Supply air dry bulb temp. (F)	TSUP	Linear thermistor	IV			IV
9	Compressor and outdoor fan energy (pulse)	DIG1	Watt-hour meter with magnetic latch pulse initiator	RT			RT
10	Indoor fan and 1st stage heater energy (pulse)	DIG2	Watt-hour meter with magnetic latch pulse initiator		CIT		RT
11	2nd stage heater energy (pulse)	DIG3	Watt-hour meter with magnetic latch pulse initiator		CIT		RT
12	Condensate metering pump (pulse)	DIG4	Positive displacement solenoid metering pump with optical coupler				RT
13	Compressor ON-OFF	MODE 0-ON	Opto-coupler	IV			IV
14	Outdoor Fan ON-OFF	MODE 3-OFF	Opto-coupler	IV			IV
15	Compressor on time for a cycle (sec)	CTIM	Clock card		CIT	CIT	
16	Defrost time for cycle (sec)	DTIM	Clock card		CIT	CIT	
17	Volumetric flow rate in return duct (ft^3/min)	FLOW	Calculated	IV			IV
18	Sensible heat (Btu)	QS	Calculated	TI	CIT	DIT	
19	Latent Heat (Btu)	QL	Calculated		CIT	DIT	
20	Compressor, outdoor fan and c.c. heater energy (Wh)	ECMP	Calculated		CIT	DIT	
21	Indoor fan energy (Wh)	EFAN	Calculated		CIT	DIT	
22	Auxiliary heaters (Wh)	EHET	Calculated		CIT	DIT	
23	Coefficient of performance	COP	Calculated		CIT	DIT	

[1] Refer to text

[2]
IV: instantaneous value
CIT: cycle integrated total
CTIA: compressor time integrated average
DIT: daily integrated total
EOC: end-of-cycle value
HSA: average of the 48 half hour scans for the day
RT: running total for a cycle
TI: value for the last time increment

complete description of the signal conditioning and computer interface system is given in Ref. 4.

3.3 Data Scanning Requirements

In order to evaluate cyclic performance it was necessary to integrate the data. This required a high data acquisition rate (especially at the start of the on-cycle) to insure accuracy. This would, however, require the storage of large amounts of data if the high acquisition rate were maintained through the cycle. Results from previous dynamic heat pump laboratory tests were reviewed to determine the optimal sliding scale of intervals between data acquisition scans. These intervals were established as (1) every 10 seconds for the first 2 minutes of a cycle, (2) every 30 seconds for the next 4 minutes, (3) every 60 seconds for the next 6 minutes, and (4) every 5 minutes until the compressor is de-energized.

3.4 Data Acquisition Format

The microcomputer was programmed to record four types of data formats scan data, cyclic data, daily data and half-hour data. 'Scan' data from each cycle were used to evaluatec instantaneous as well as overall cycle performance. The performance summary of each cycle is referrred to 'cyclic' data. Cyclic data were recorded on disk for each cycle. In addition, a complete set of scan data was recorded for every one out of ten cycles (i.e., 10 percent of all scan results are available for further analysis). The purpose of this was to provide disk space for other types of data and not fill it with redundant information since only 'typical' cycles and accumulated data were of interest. 'Cyclic' data for each day were processed using summation and/or averaging techniques. Results were recorded on disk at the end of each day. Daily

performance summaries are referred to as 'daily' data. Daily data include 24-hour integrated totals of cooling done and electrical energy requirements as well as average outdoor temperature for the 24-hour period. Half-hourly measurements of the indoor and outdoor air temperatures were also recorded, irrespective of the operation of the unit and referred to as 'half-hour' data.

Approximately twelve types of data were recorded for each of the four data formats: scan, cyclic, daily, half-hour. These four data formats, the type of data record in each format and a description of how each data value is determined, are indicated in Table 3.1. Printouts and further analysis of these data were made using the central microcomputer located at NBS.

4. DATA DISCRIMINATION AND FIELD TEST SUMMARY

An overview of the operation and thermal performance of each of the three field-located heat pumps for the 1980 cooling season is given in Table 4.1. The data recording period is presented in lines 2 and 3. Comparing the data collection period in line 3 with the number of hours in which reliable data were recorded and available for analysis (line 7) indicates a significant loss in data collection, due to a number of factors. Early in the data collection period, the condensate metering system was not functioning properly and the cooling data, therefore, was not complete for that period. Also, the units were turned off occasionally when cooling was not required. The time which units 1, 2 and 3 were switched off were 9 percent, 30 percent, and 9 percent, respectively, of the total cooling season data collection period. Some data were also lost due to late replacement of data saturated disks. Lost data amounted to 16 percent, 11 percent, and 6 percent of the total data collection period for units 1, 2, and 3, respectively.

In the process of reviewing the data, additional cycles were excluded from analysis. These excluded cycles included (1) cycles initiated manually by adjustment of the thermostat setting to some value lower than that of the previous cycle, (2) cycles aborted manually by adjustment of the thermostat setting to some value higher than that which initiated the cycle, and (3) other cycles in which manual adjustment did not alter the compressor operation mode, but nonetheless resulted in detectable changes in return air temperature in subsequent operation. These cycles were readily detected as they had either (1) extended compressor-on periods relative to the preceeding cycle, or (2) extended compressor-off periods relative to the preceeding cycle. It was felt that the above cycles were unduly influenced by individual human

Table 4.1 Overview of Seasonal Cooling Performance

Comparison of Three Field Units

	ITEM	UNIT 1	UNIT 2	UNIT 3
1	Nominal Capacity	2 1/2 ton	3 ton	3 ton
2	Cooling season data collection period	6/15/80 to 9/25/80	6/15/80 to 10/2/80	6/17/80 to 9/14/80
3	Day numbers	167 to 269	167 to 276	169 to 258
4	Total cycles n	1113	885	446
5	Total compressor time TCTIM (hrs)	221	287	168
6	Avg. Comp. time $\bar{t}_{on}$ (min/cyc)	11.9	19.5	21.6
7	Total cycle time TTIM (hrs)	671	599	646
8	Avg. cycle time (min/cyc)	36.2	40.6	83.2
9	TCTIM/TTIM = t_{on}/τ	.329	.479	.260
10	QS (Btu) x 10^{-6}	4.823	5.433	3.670
11	QL (Btu) x 10^{-6}	1.012	1.110	1.059
12	QS + QL = (Btu) x 10^{-6}	5.835	6.543	4.729
13	QS/Q	.827	.830	.775
14	Avg. capacity Q = Q/TCTIM (Btu/hr)	26400	22800	28200
15	Q/N (Btu/cycle)	5240	7390	10100
16	Avg. Load L = Q/TTIM (Btu/hr)	8690	10900	7150
17	Compressor energy WCOMP (kWh)	819	829	627
18	Indoor fan energy WFAN (kWh)	115	197	81
19	Total Energy W (kWh)	934	1089	708
20	$\dot{W}$ = W/TCTIM (W)	4226	3794	3732
21	W/N (kWh/cyc)	.839	1.23	1.52
22	Seasonal EER	6.25	6.01	6.68

preference (such as windows and doors left open) which, if included, would make generalizations difficult.

Early in the study, a method was developed to filter out the effects of manual resets of the thermostat. A simple criterion which detected changes in return duct air temperature, TRET, by an amount, ΔTRET, was established to determine whether or not a given cycle, n, was affected by a manual reset of the thermostat. If for each cycle, n, and subsequent cycle (n + 1):

$$\left| \text{TRET}\ (n+1) - \text{TRET}\ (n) \right| > \Delta\text{TRET},$$

then cycles n and n + 1 were deleted. The magnitude of ΔTRET was established by analyzing the values of TRET where manual changes in thermostat setting were known not to have occurred. This analysis found specific thermostat operating differentials for each unit resulting in the following limits for ΔTRET:

UNIT	ΔTRET
1	0.5°F
2	1.0°F
3	1.0°F

5. STEADY-STATE FIELD PERFORMANCE

5.1 Weather

Since field data for the three units were gathered over different portions of the cooling season, the number of hours for a given outdoor temperature range varied. Table 5.1 lists the fraction of temperature bin hours, n_j/N, for each temperature bin, T_j, during the test periods for the three units.

Table 5.1 Fraction of Total Number of Temperature Bin Hours During the Test Period

Range of T_{out} (°F)	Decimal Fraction of 1980 Cooling Season Hours Unit #1	Unit #2	Unit #3
55-60	0	0	0
60-65	.0143	.0	.0553
65-70	.1047	.1150	.2267
70-75	.2014	.2545	.2501
75-80	.1557	.2366	.1855
80-85	.1292	.2656	.1682
85-90	.1806	.1272	.1024
90-95	.1647	.0011	.0119
95-100	.0494	0	0
Total Test period hours, N	671.5	598.8	645.9

In subsequent discussions, the cooling performance results over the test periods are referred to as seasonal cooling performance results. It should be noted that intercomparison of seasonal performance results between units is limited since the fraction of outdoor temperature bin hours are different.

5.2 Steady-State Results

The steady-state part load performance results were obtained from the (detailed) scan data. The term 'steady-state part-load' is used in the sense that the unit is operating steadily but at less than peak capacity due to variations in the indoor humidity and indoor and outdoor ambient temperatures. The number of cycles of scan data available for steady-state analyses are listed below along with the total number of cycles for the test periods of the three units. To evaluate the part load steady-state sensible cooling capacity and power from the scan data, data from the first 5 to 8 minutes after a unit cycled on was disregarded. Data from the remaining time until unit shut-down was found to be relatively unchanging and could be used to determine the steady-state performance.

	Scan Data Cycles	Total Number of Cycles
Unit 1	101	1113
Unit 2	77	885
Unit 3	40	466

Since condensate was collected only at the end of a complete on-off cycle, it was necessary to estimate the steady-state latent capacity. Two different methods were used in obtaining the estimate. The first method assumed that the ratio of latent to sensible capacity was the same for the entire cycle and steady-state portion of the cycle. This is expressed as follows:

$$\frac{\dot{Q}^{\ell}_{ss}}{\dot{Q}^{s}_{ss}} = \frac{\dot{Q}^{\ell}_{cyc}}{\dot{Q}^{s}_{cyc}} = \text{constant} \qquad (5.1)$$

The quantities $\dot{Q}^{\ell}_{ss}$ and $\dot{Q}^{s}_{ss}$ denote latent and sensible steady-state capacities respectively and $\dot{Q}^{\ell}_{cyc}$ and $\dot{Q}^{s}_{cyc}$ the latent and sensible cooling done over a complete cycle.

Steady-state performance results versus outdoor temperature for the three field units are presented in figures 5.1, 5.2 and 5.3. The results are averaged values over all the scan cycles for a given temperature bin.

Although the steady-state part load capacity and efficiency would be expected to decrease smoothly with increasing outdoor temperature, the results of figures 5.1 and 5.3 show erratic behavior. This behavior is due in part to variations in the return air wet-bulb and dry-bulb temperatures which must also be considered (Carnot effect due to changes in source and sink temperatures).

An example of typical results presented in figure 5.4 provide a clue for another cause for the erratic behavior in the steady-state part load performance results. As the figure demonstrates at a given outdoor temperature, the steady-state capacity tends to increase with increasing cycle on-time. This behavior was found to occur for all three units.

The reason for the dependence of the steady-state performance on length of cycle on-time may be traced back to the assumption discussed earlier and embodied by equation (5.1). An improved estimate for the steady-state latent capacity can be obtained by noting that condensate will generally not be generated at a steady-state rate until several minutes after the cooling unit

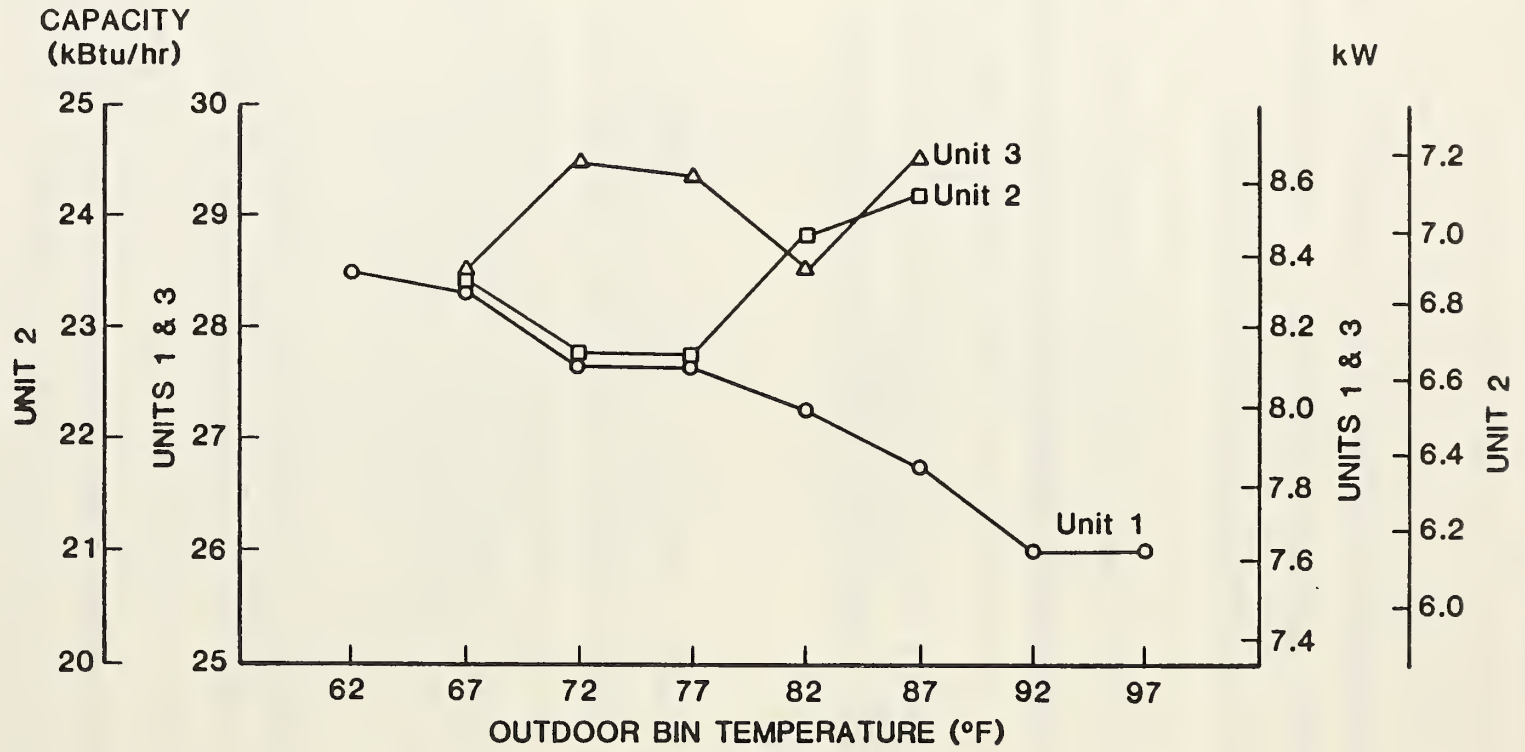

Figure 5.1. Part load steady-state field performance
[Capacity vs. outdoor bin temperature results, °F].

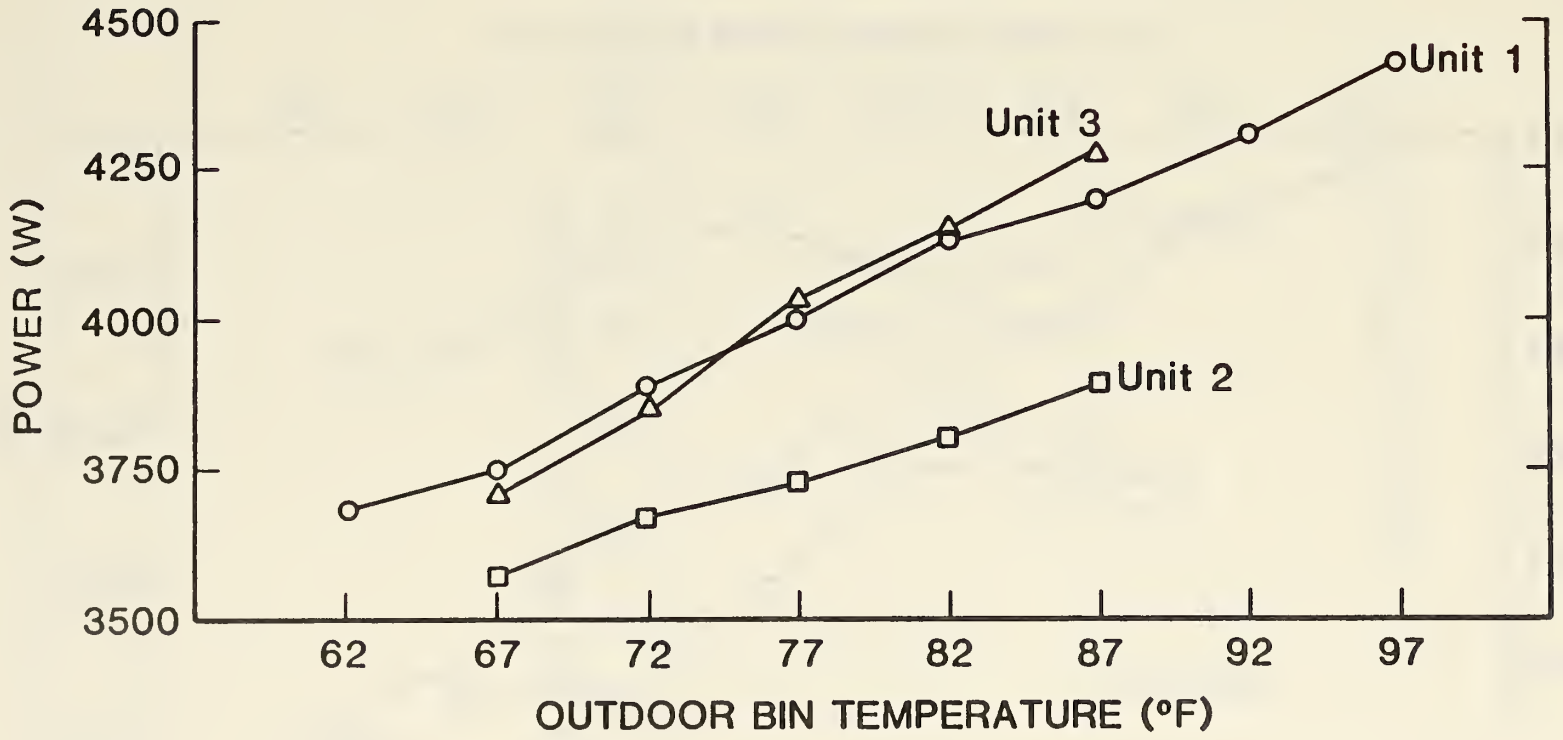

Figure 5.2. Part load steady-state field performance results [Power vs. outdoor bin temperature, °F].

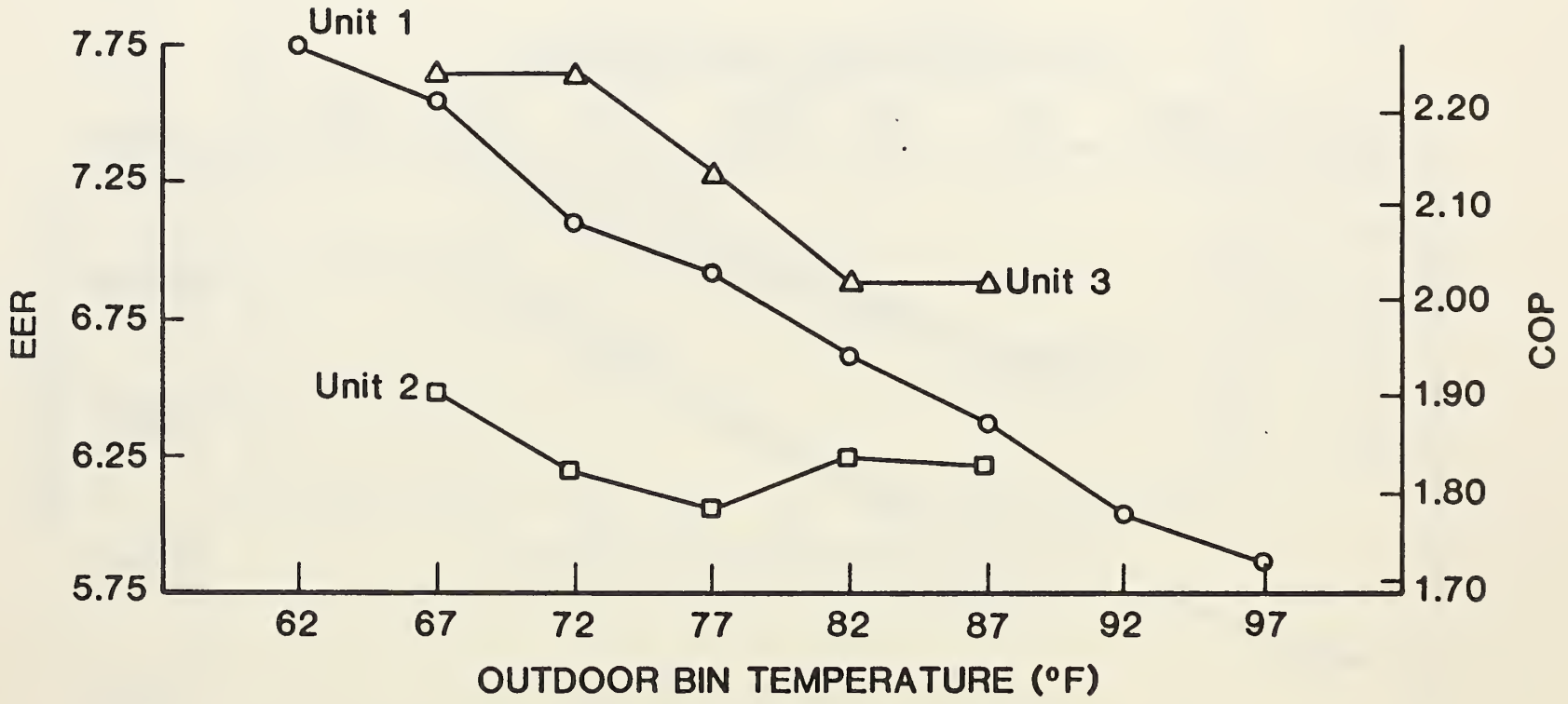

Figure 5.3. Part load steady-state field performance results [EER and COP vs. outdoor bin temperature, °F].

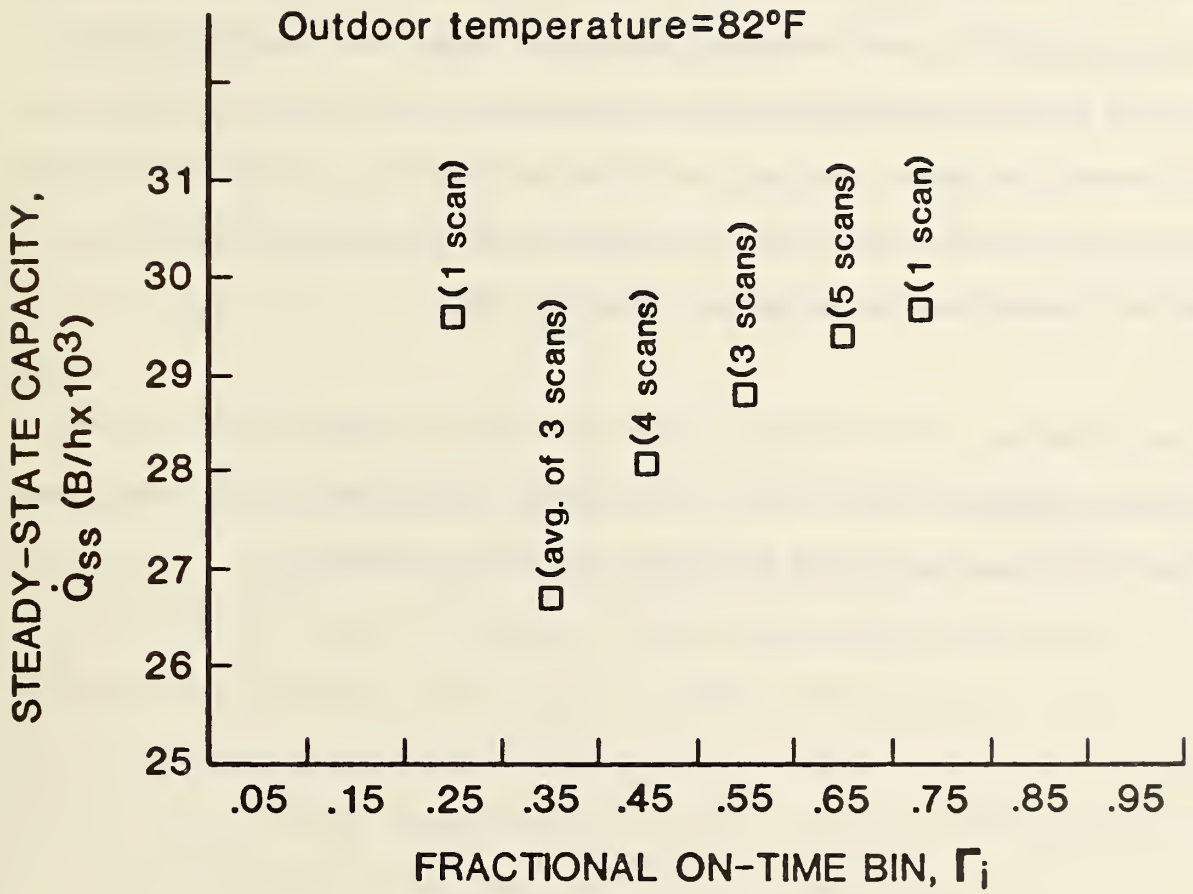

Figure 5.4. Steady-state capacity versus fractional on-time, unit 3.

cycles on. To account for this, equation (5.1) is modified to the following form:

$$\frac{\dot{Q}^{\ell}_{ss}}{\dot{Q}^{s}_{ss}} = \frac{Q^{\ell}_{cyc}/(t_{on} - c)}{Q^{s}_{cyc}/t_{on}} \tag{5.2}$$

where t_{on} denotes the total cycle on-time and c is the time required (ranging from 2 to 4 minutes as found in laboratory tests) after the unit cycles on, for condensate to form on the coil and to be generated at a steady-state rate. A more complete discussion is given in Appendix A.2 and subsequent results include the assumptions summarized by equation (5.2).

It is worth noting that the above expression predicts higher latent and total steady-state capacities than would be obtained by equation (5.1) for short on-time and exhibiting negligible difference for larger on-times.

6. CYCLIC PERFORMANCE

6.1 Overview of Seasonal Cooling Requirements and Unit Sizing

The percentage of total seasonal cooling requirements versus outdoor temperature of the residences associated with the three field units is presented in figure 6.1. For the residences associated with units 2 and 3 the histogram is bell-shaped, centering around an outdoor temperature of 82°F. Unit 1 has a flatter profile with the greatest percentage of cooling occurring in the range of 87°F to 92°F. The shape of the histograms reflect several factors including outdoor temperature-generated heat gains, solar heat gain, occupancy usage patterns (internal heat gains) as well as the building shell.

Seasonal building cooling load curves can be derived from the data presented in figure 6.1 together with the temperature bin hours presented in Table 5.1. These curves are shown in figure 6.2. The figure demonstrates that a heat pump unit may encounter a wide range of cooling load profiles. Since the relationship between building load and outdoor temperature varies from house to house, the seasonal energy efficiency ratio of a given unit can also vary even if the temperature bin hours and sizing are identical.

In order to fully account for the building seasonal cooling load profiles presented in figure 6.2 a detailed (computerized) analyses is required and is beyond the scope of this report. Nevertheless, several factors can be identified which qualitatively explain the curves. One obvious factor affecting the shape of the curves is the strategic location of the thermostat and the placement and operation of the registers which can lead to significant

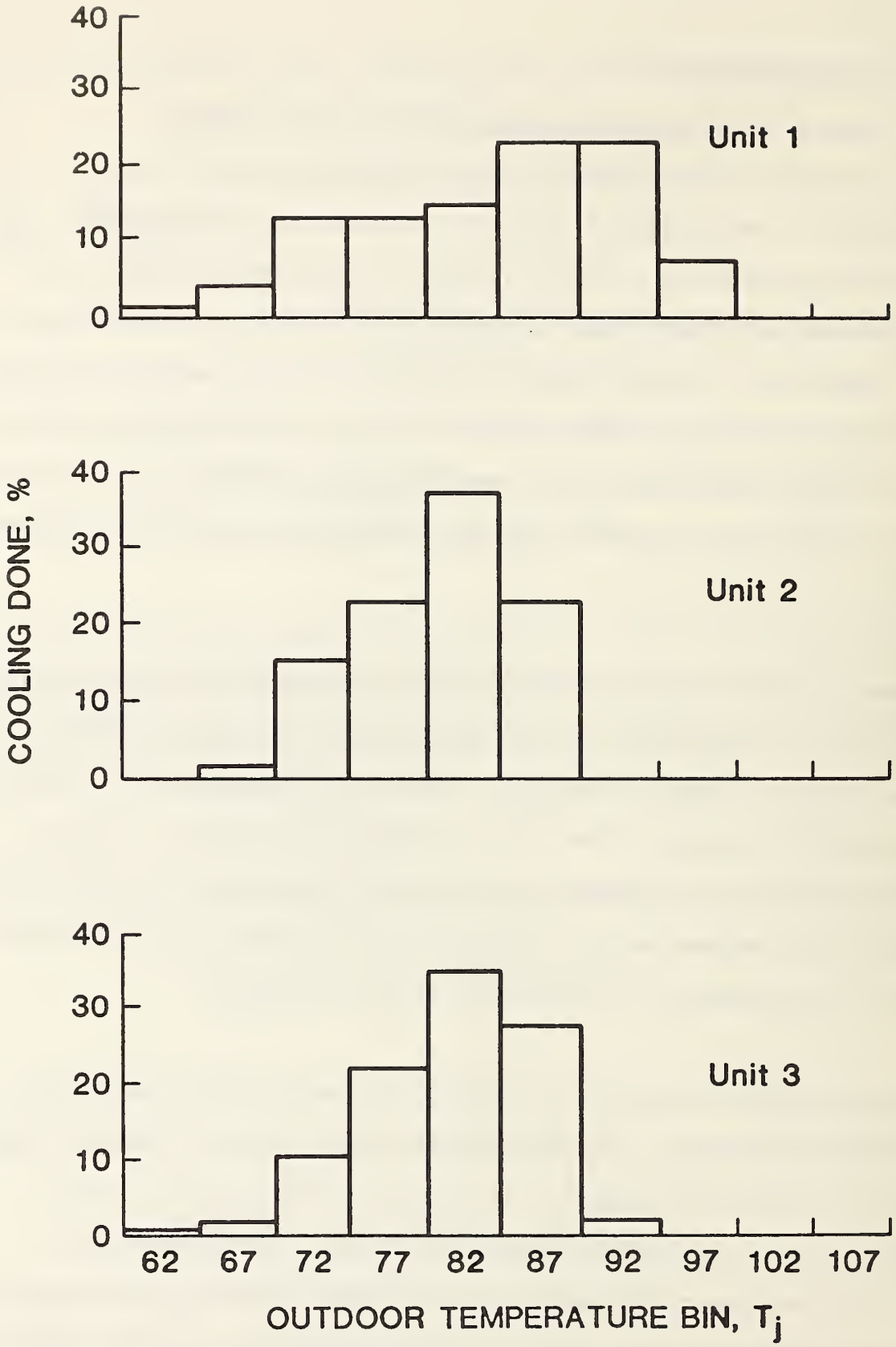

Figure 6.1. Percent seasonal cooling done versus outdoor temperature.

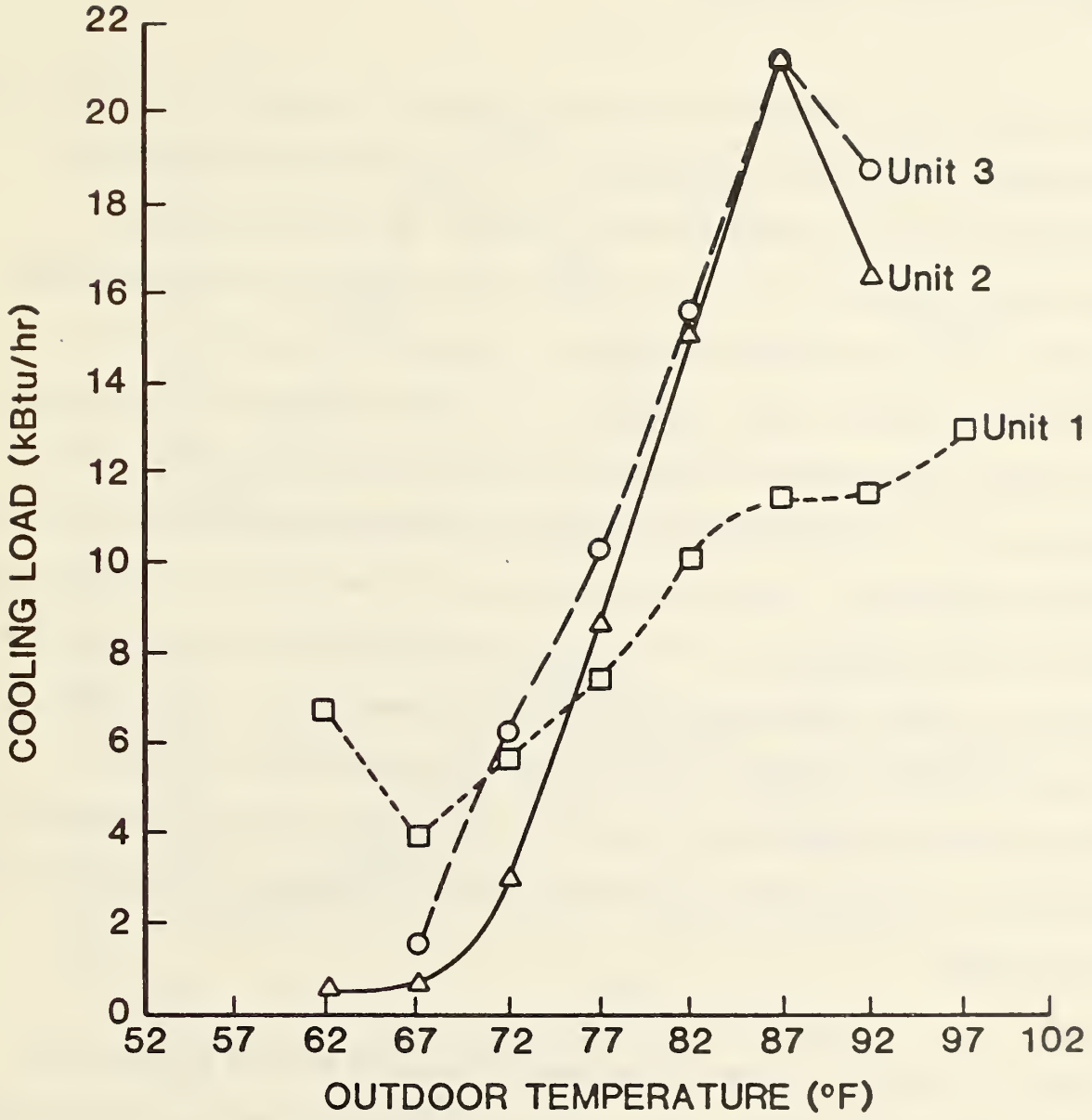

Figure 6.2. Seasonal average cooling load profiles for three field installations.

indoor air temperature stratification and false indications of the total household cooling requirements.

The building load associated with unit 1 exhibits a somewhat flat profile with the outdoor temperature. The structure was of a relatively heavy brick construction with an underground and frequently used basement. This construction would tend to act as a heat sink, minimizing the instantaneous effects of solar and outdoor temperature generated heat gains. The two remaining residences (units 2 and 3) show a steeper cooling load slope up to an outdoor temperature of 87°F beyond which the load tends to level off or decrease. The residences were of a lighter wood frame construction and with walk-out basements. In one case the basement was not used as living quarters. With the relatively light construction the observed drop in the cooling load beyond an outdoor temperature of 87°F could be due in part to the short thermal response delay from that time in the afternoon when outdoor temperatures are highest to a later time when outdoor temperatures would be expected to be lower and occupancy rates and (instantaneous) internal heat gains higher.

Figure 6.3 presents results of the percent seasonal cooling done and the percentage of total cycles as a function of fractional on-time. Of the three units, unit 1 is the most oversized since it exhibits the greatest percentage of seasonal cooling and cycling at fractional on-times below .45. During the test period the unit never exceeded a fractional on-time beyond .65. Unit 2 appears to be properly sized with a large percentage of cooling done at fractional on-times exceeding .55. The relative sizing for unit 3 lies between units 1 and 2 with the greatest amount of cooling provided at

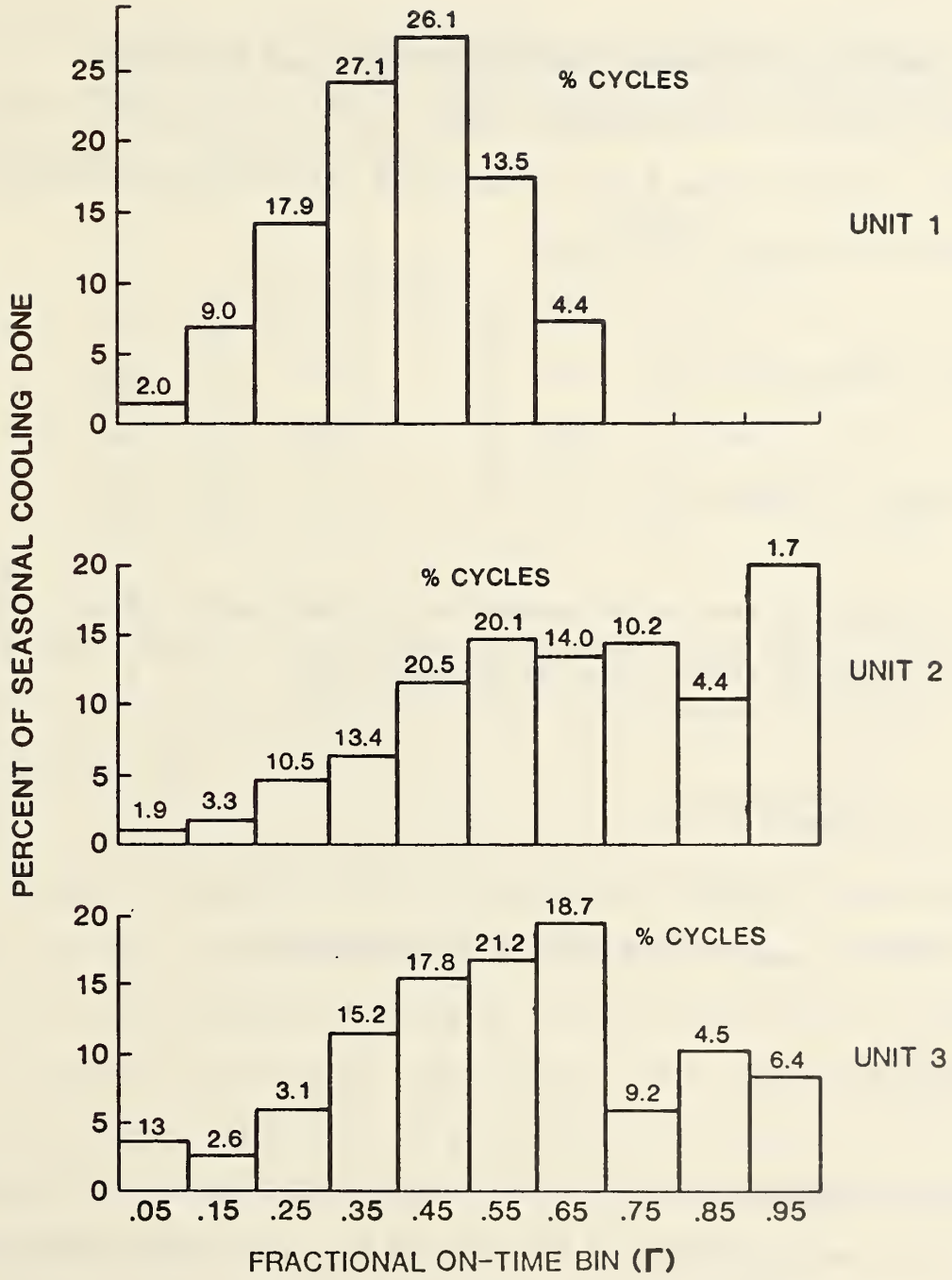

Figure 6.3. Percent seasonal cooling done and percent of total cycles versus fractional on-time, Γ.

fractional on-time ranging from .45 to .65. Oversizing on cooling will degrade unit cyclic performance as well as providing less control in maintaining proper dehumidification.

6.2 Comparison of Thermostat Model Predictions and Field Data

The development of the thermostat model is given in Appendix A.1. The model predicts a cycling rate, N, as a function of the fractional on-time, Γ, through the following expression:

$$N = 4\, N_{max}\, \Gamma\, (1 - \Gamma) \tag{6.1}$$

where N_{max} = cycling rate at $\Gamma = 0.5$

Since the cycling rate is the inverse of the total cycle time, τ, the above expression may be used to find the on-time, t_{on}:

$$t_{on} = \frac{1}{4N_{max}(1 - \Gamma)} \tag{6.2a}$$

The off-time, t_{off}, is then given by the expression

$$t_{off} = \tau - t_{on} \tag{6.2b}$$

In order to obtain a good fit of equation (6.1) to the data, it was necessary to obtain a good estimate for the value of N_{max}. This was accomplished by calculating N_{max} from equation (6.1), utilizing values of N and Γ obtained from the data. The data used in calculating N_{max} ranged from $\Gamma = .25$ to

Γ = .75 to incorporate the statistically more significant number of cycles. An average value of N_{max} was then determined for each unit.

As seen in figures 6.4(a), (b) and (c) the model is in excellent agreement with the data. Values of N_{max} for the three units are given below along with corresponding on-off times for Γ = 0.2.

		Γ = 0.2	
	N_{max}(cycles/hr)	t_{on}(min)	t_{off}(min)
Unit 1	2.13	8.8	35.2
Unit 2	2.28	8.2	32.9
Unit 3	1.64	11.4	45.8

The above results indicate a significant increase in the on-time at Γ = 0.2 as compared to the on-off time (6/24) used in the test procedures for cyclic cooling performance (3).

Figure 6.4 presents a comparison of the semi-empirical thermostat model with experimental results. The average values of fractional on-times, Γ, and cycling rates, N, were obtained by averaging over the total number of cycles in the test period for each fractional on-time bin. Also illustrated in the figure is the standard deviation of the data, obtained by assuming that all cycles falling within a given fractional on-time and outdoor temperature bin have approximately equal fractional on-times and cycling rates.

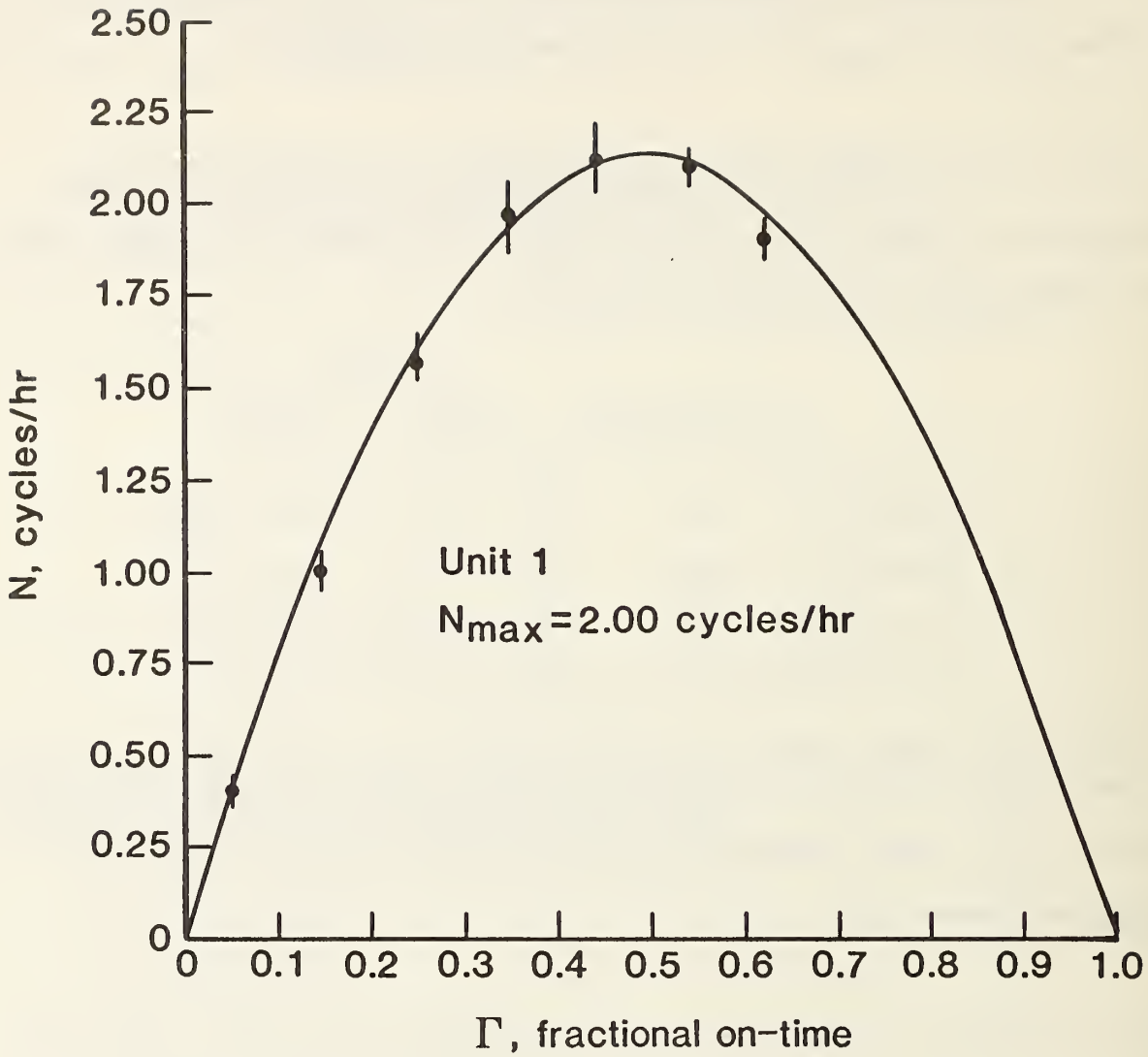

Figure 6.4(a). Comparison of the thermostat model with field data [Unit 1].

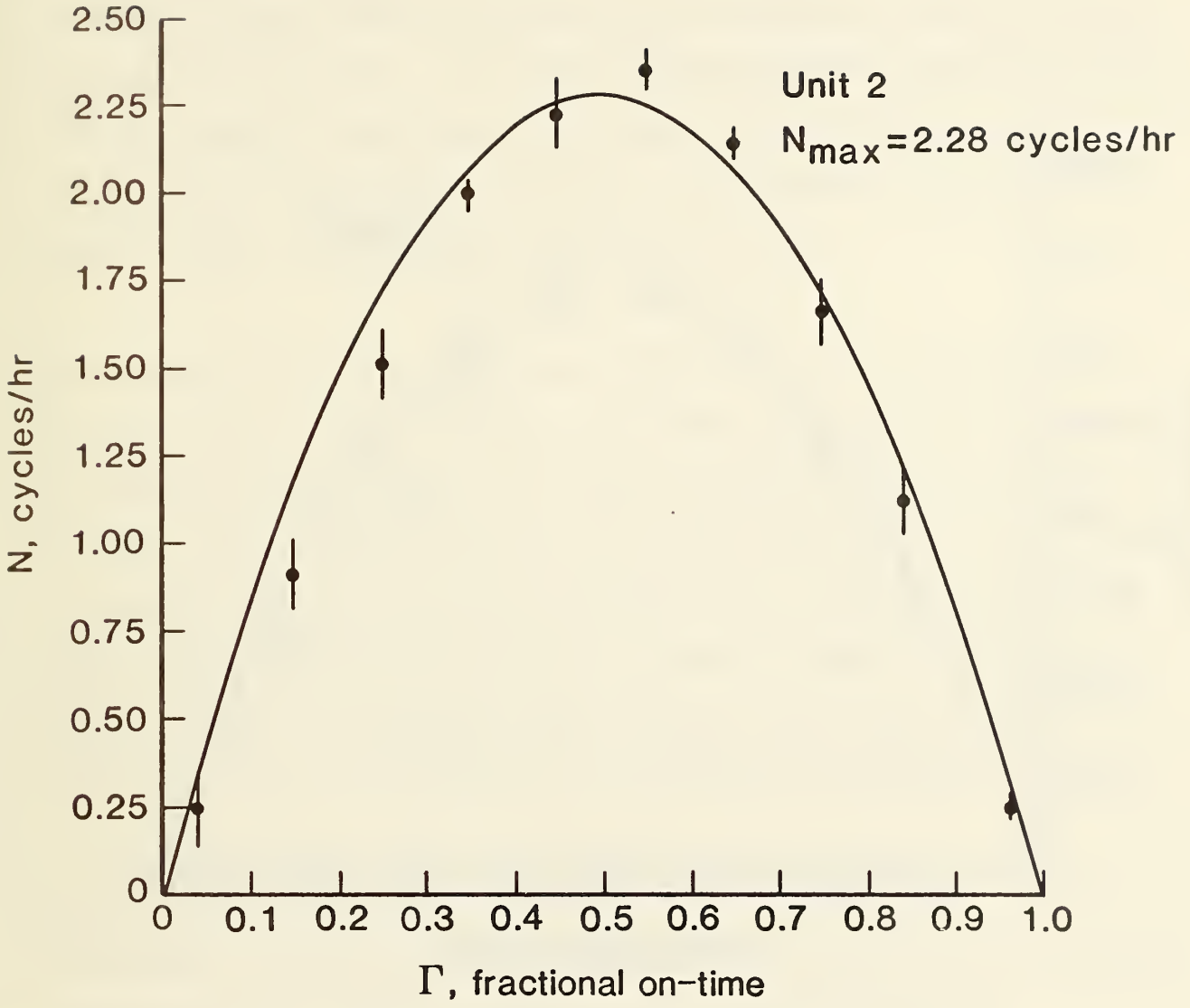

Figure 6.4(b). Comparison of the thermostat model with field data [Unit 2].

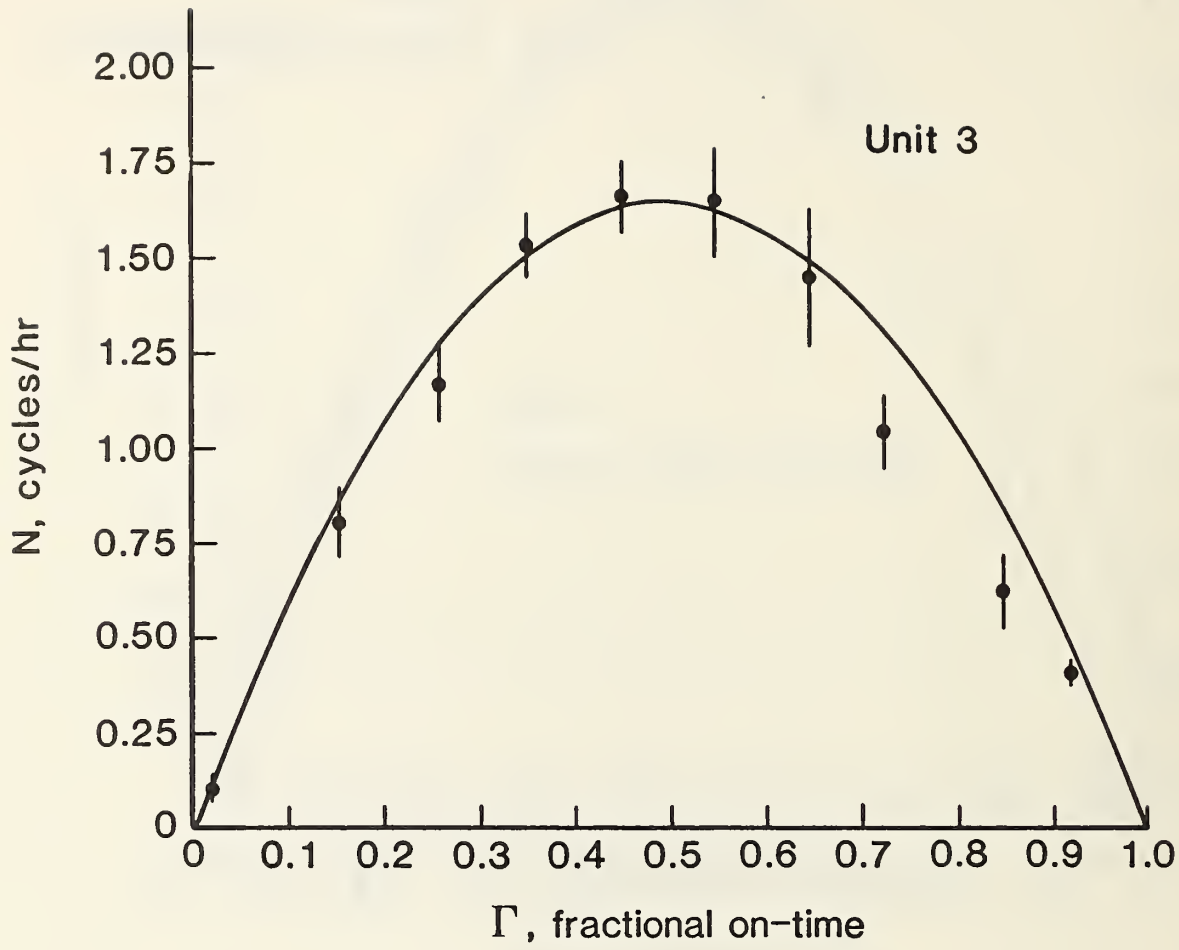

Figure 6.4(c). Comparison of the thermostat model with field data [Unit 3].

6.3 Cyclic Performance Parameters

6.3.1. Data Organization

The field data were organized into 5°F outdoor temperature bins, T_j, and .10 fractional on-time bins, Γ_i. The types of data organized in this manner were cooling consumption, energy used, cycle period, number of cycles, cooling load factors and part-load factors. These data were summed or averaged over the number of cycles, k (as appropriate) for each i, j bin.

As discussed in Section 3.4, two major types of data were collected and primarily used in the data analyses. The first type is referred as cycle data in which only the total capacities, $\dot{Q}_{cyc,ij}$ and power used, $\dot{W}_{cyc,ij}$ were recorded. The cycle data consisted of all cycles undergone by the units which were used for evaluating seasonal performance. The second (a subset of the first type) is referred to as scan data. These data include portions of a cycle from which steady-state capacities, $\dot{Q}_{ss,ij}$, power $\dot{W}_{ss,ij}$, cooling load factors, CLF_{ij} and part-load factors, PLF_{ij} could be calculated.

6.3.2 Determination of the Cooling Load and Part Load Factors

As discussed in Section 5.2, steady-state sensible capacity and power could be evaluated from scan data by using only those data collected after approximately the first 5 to 8 minutes after unit start-up. For each cycle falling within a given fractional on-time bin Γ_i and outdoor temperature bin, T_j, the part load and cooling load factors were obtained by the expressions:

$$CLF_{ij} = \frac{Q_{cyc,ij}}{\dot{Q}_{ss,ij}} \frac{1}{\tau_{ij}} \qquad (6.3)$$

$$PLF_{ij} = \frac{EER_{cyc,ij}}{EER_{ss,ij}} \tag{6.4}$$

where τ_{ij} denotes the length of the on-off cycle.

As noted in Section 5.2, two methods were used to estimate the steady-state latent capacity from the total condensate collected in a cycle. The steady-state latent capacity could be determined from the following expression:

$$\dot{Q}^{\ell}_{ss,ij} = \dot{Q}^{s}_{ss,ij} \frac{Q^{\ell}_{cyc,ij}/(t_{on,ij} - c)}{Q^{s}_{cyc,ij}/t_{on,ij}} \tag{6.5}$$

where the superscripts s and ℓ denote sensible and latent respectively and t_{on} is the total on-time for a given cycle. All the quantities on the right-hand side of equation (6.5) (except the value c) are measured. The value c is the time required after unit start-up for condensate to form on the coil and be generated at a steady-state rate. Values of c = 0,2,3,4 minutes are used throughout this report. Results obtained from laboratory tests indicate that a reasonable estimate is c = 2 minutes. Appendix A.2 outlines the derivations in obtaining PLF and CLF for $c \neq 0$ from values obtained for c = 0.

6.3.3 Cyclic Performance Results

In reviewing the scan data for the three field units it was noted that for any given frational on-time bin, Γ_i, the cooling load factor, CLF_{ij} and part load factor, PLF_{ij}, were insensitive to the outdoor temperature bin, T_j. A typical example of the results is given in figure 6.5. This result simplified

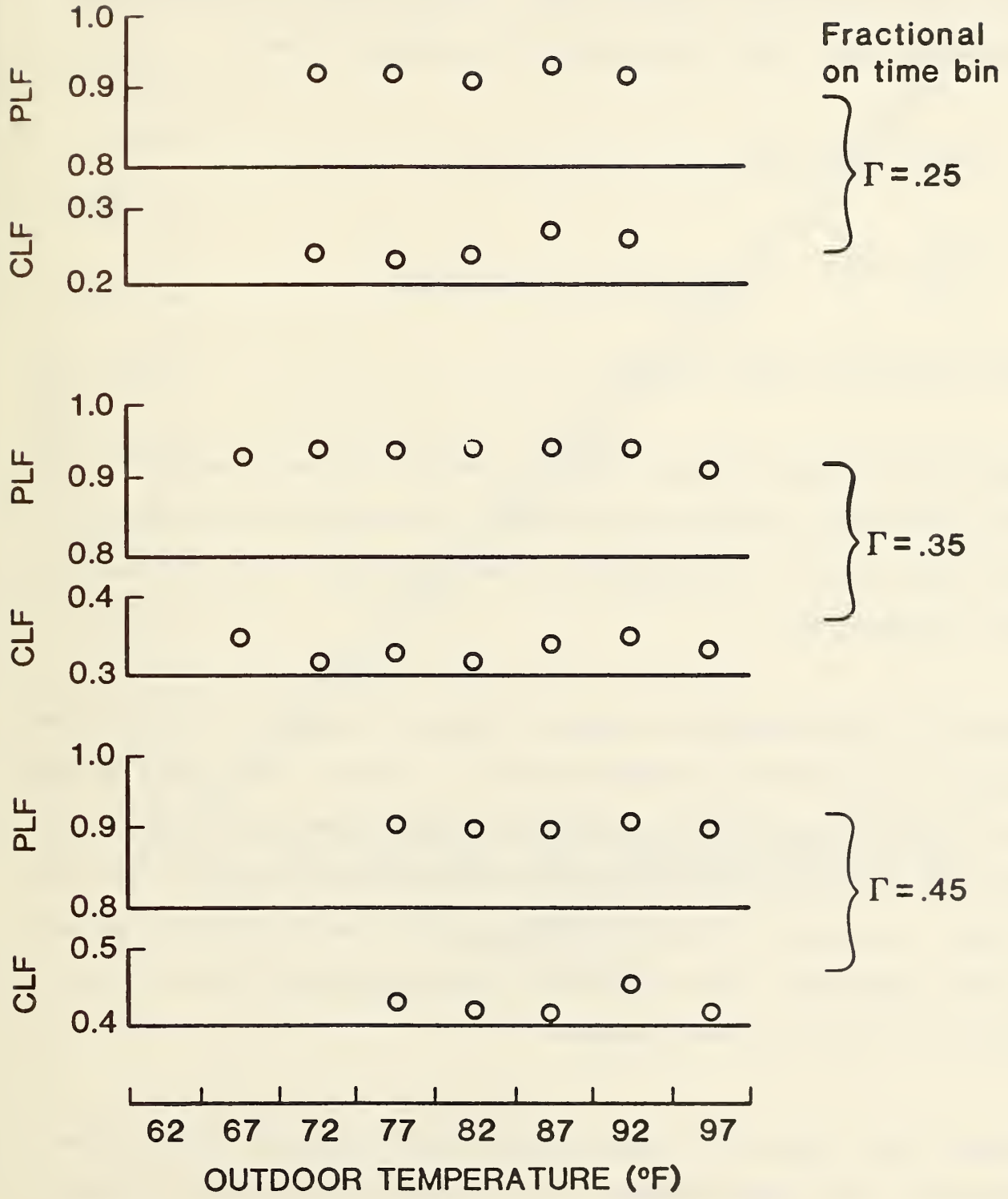

Figure 6.5. Cooling load factors and part load factors for selected fractional on-time bins versus outdoor temperature; typical results (unit 1).

subsequent seasonal field performance calculations. In addition, the result is in agreement with previous laboratory results and implicit in the seasonal performance calculations required of heat pump and central air-conditioners manufacturers [3]. This result may also be stated as follows:

$$CLF_{ij} = CLF_i, \text{ and}$$
$$PLF_{ij} = PLF_i \qquad (6.6)$$

and is employed in later sections.

Figure 6.6 illustrates typical results of cooling load factor versus fractional on-time. Due to part load losses, the curve deviates from the ideal curve: $CLF = \Gamma$. As expected, at the end points $\Gamma = 0,1$, CLF tends to 0 and 1, respectively.

Results for PLF versus CLF are given in figures 6.7 and 6.8. Figure 6.7 shows typical results of PLF versus CLF for unit 3. As seen in the figure, the part load data are very consistent, exhibiting a small standard deviation of $\pm$ .02. Some data do not show deviation marks since they contain only one or two data points. The standard deviations in PLF for units 1 and 2 averaged $\pm$ .02 and $\pm$ .035, respectively. These deviations remain approximately the same for values of c = 0, 2, 3, and 4 minutes.

Figures 6.8(a), (b) and (c) contains graphs of PLF versus CLF for the three units for c = 0, 2, and 4 minutes. It is evident from the graphs that at a constant CLF, PLF decreases for increasing values of c. This is expected

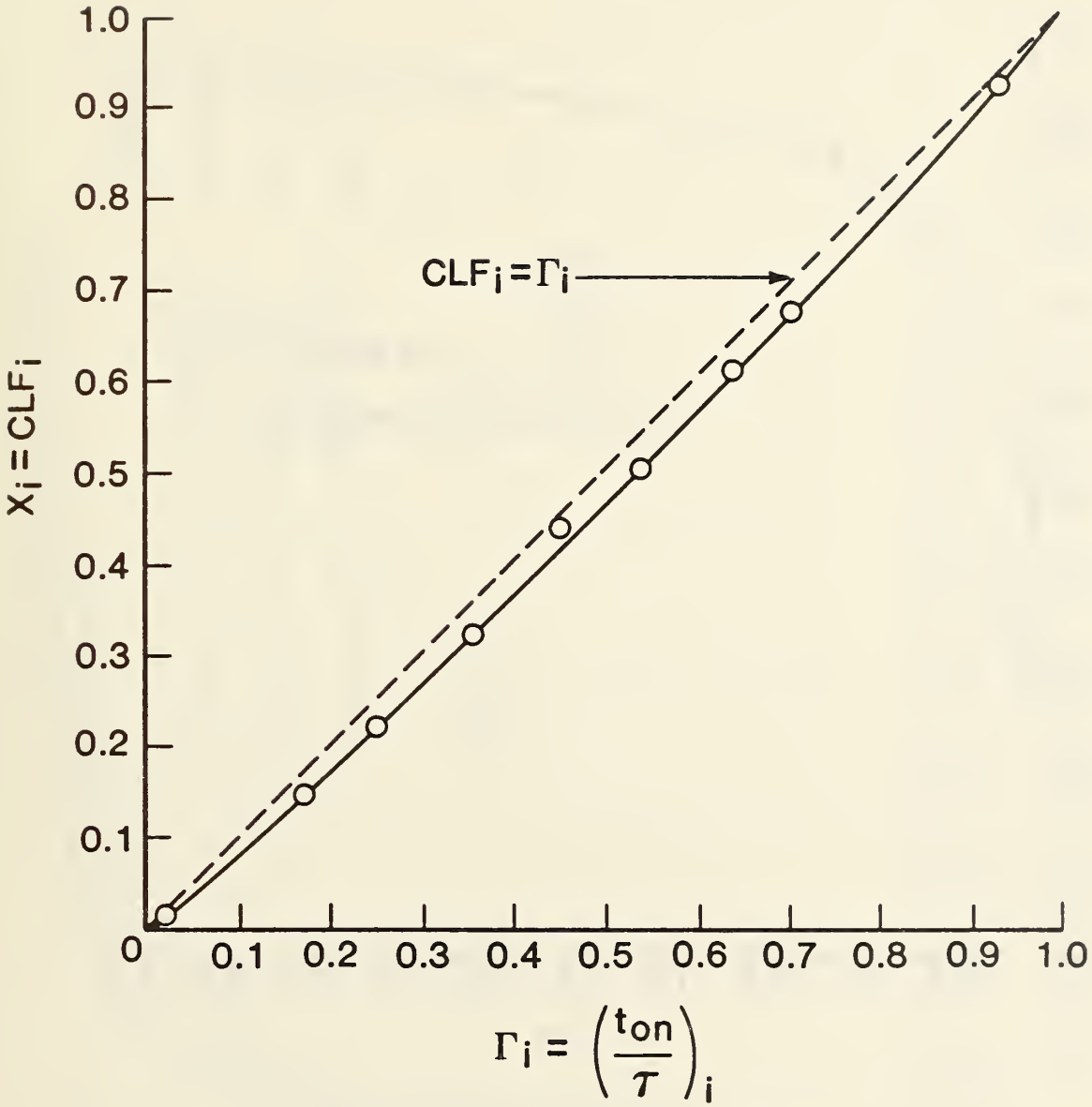

Figure 6.6. Cooling load factor versus fractional on-time for Unit 3 (c = 0 min).

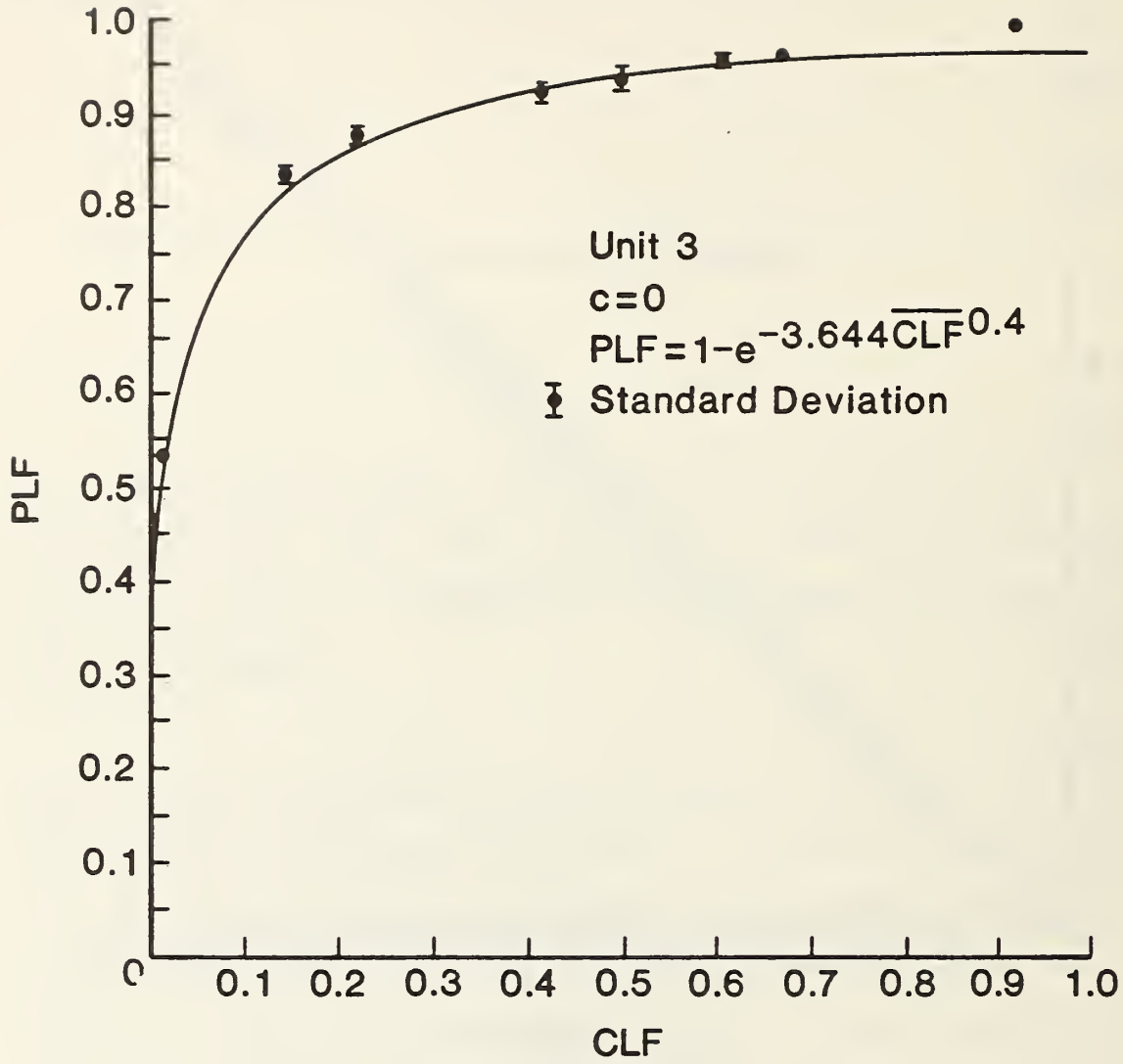

Figure 6.7. Comparison of empirical curve with the mean and dispersion of data--typical data.

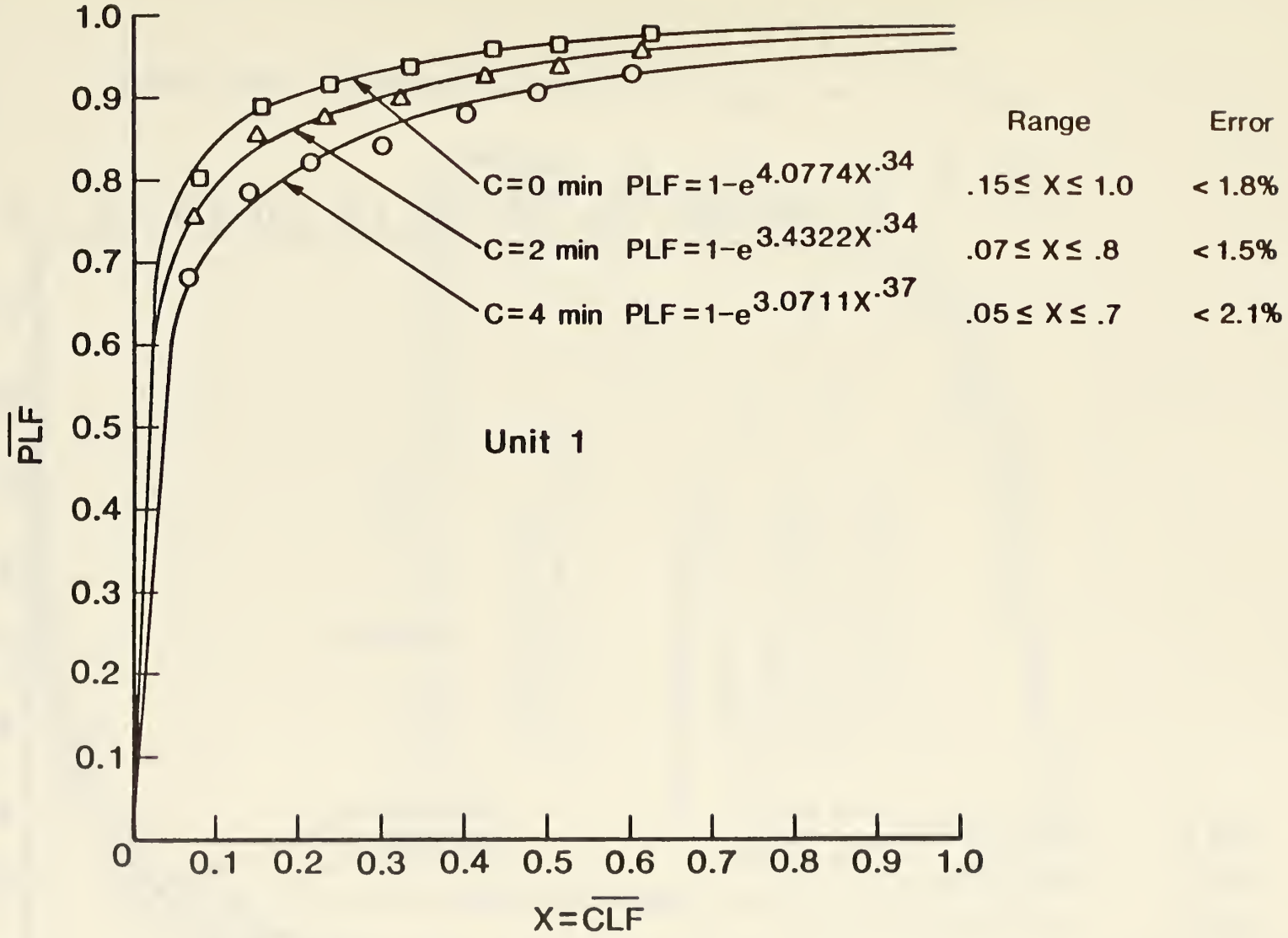

Figure 6.8(a). Comparison of data and empirical curve fit [Unit 1].

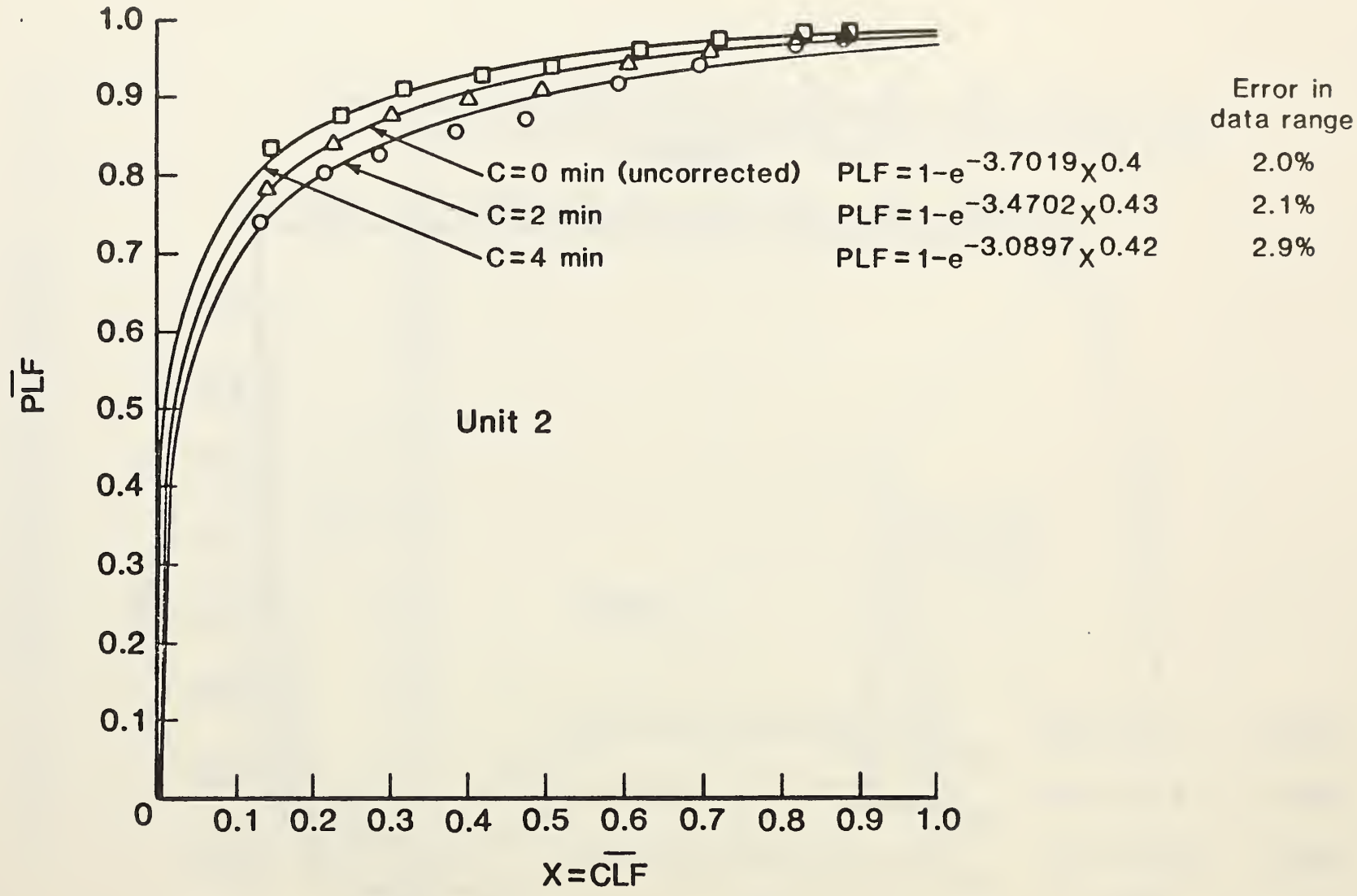

Figure 6.8(b). Comparison of data and empirical curve fit [Unit 2].

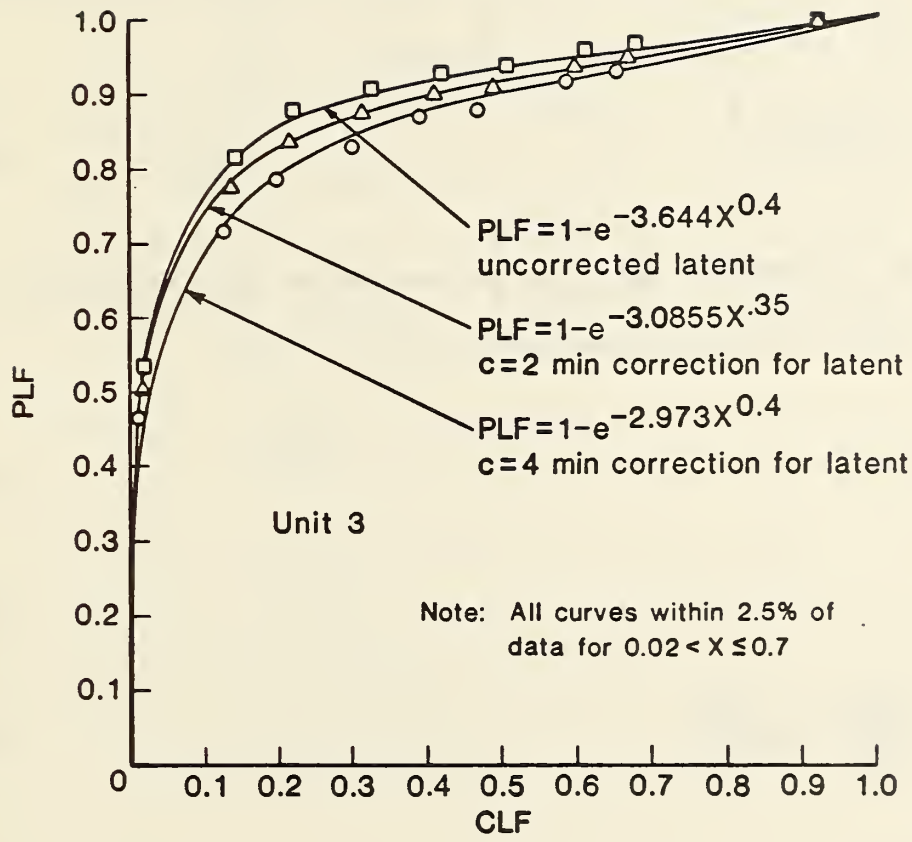

Figure 6.8(c). Comparison of data and empirical curve fit [Unit 3].

since increasing values of c result in increasing values of the steady-state latent and total capacities. The resulting ratio of EER_{cyc} and EER_{ss} therefore decreases.

Empirical curves were fitted to the data of figure 6.8 and had the following form:

$$PLF = 1 - e^{-p(CLF)q} \tag{6.7}$$

In evaluating the constants p and q the above equation was linearized to the form:

$$\eta_i = a + q\,\varepsilon_i \tag{6.8a}$$

where $p = e^a$ (6.8b)

$$\eta_i = \ln \ln\left\{\left[\frac{1}{1 - PLF_i}\right]\right\} \tag{6.8c}$$

$$\varepsilon_i = \ln [CLF_i] \tag{6.8d}$$

A least square fit of the data (denoted by the subscript i) in the form of equation (6.8) was taken over a selected range (generally over the range CLF = .1 to CLF = .6) to evaluate the constants p, q. Table 6.1 contains values for p and q for the three units.

Table 6.1 Values for Part Load Performance Constants, p, q for the Three Units*

	UNIT 1		UNIT 2		UNIT 3	
	p	q	p	q	p	q
c = 0 min	4.0774	.34	3.7019	.40	3.644	.40
c = 2 min	3.4822	.34	3.4702	.43	3.0855	.35
c = 3 min	3.265	.35	3.320	.44	3.1997	.415
c = 4 min	3.0811	.37	3.0897	.42	2.973	.40

*$PLF = 1 - e^{-p(CLF)q}$

It is evident from figure 6.8 that the curves fit the data surprisingly well. For values of CLF ranging from .1 to .8 the average deviation of the curve from the data was 0.5 percent with a maximum error of 2.9 percent. For values of CLF less than .1, the error ranged from 2 percent to 14 percent. In this range, however, very little data were available to obtain an accurate value for PLF. For values of CLF ranging from .8 to 1.0, the error averaged approximately 3 percent with a maximum of 4.8 percent. These errors occurred mostly at the value of CLF = 1 where equation (6.7) predicts a value less than unity for PLF.

The above curves were used in the seasonal performance calculation of the three units. Although the error for very small values of CLF appeared significant, it was considered unimportant since very little cooling was done in this part of the range. For values of CLF ranging from .7 to 1.0, a straight line was used, joining the curve fit at CLF = .7 and having a value of PLF equal to 1 at CLF = 1. This piecewise curve fit was used since the exponential portion resulted in values of PLF slightly less than 1 at CLF = 1.

7. SEASONAL PERFORMANCE EVALUATION

The seasonal part load factor is defined as:

$$PLF_{seas} = \frac{SEER}{SEER_{ss}} \tag{7.1}$$

where:

$$SEER = \frac{Q}{W} \tag{7.2}$$

$$SEER_{ss} = \frac{Q}{W_{ss}} \tag{7.3}$$

and Q = the total cooling done over the test period

W = the total electrical energy used over the test period

W_{ss} = the total electrical energy that would have been used over the test period had the unit operated with no part load losses.

A straight-forward method for determining W_{ss} would be to use the steady-state results presented in figure 5.2 for each temperature bin, T_j. $W_{ss,j}$ could then be determined from the following expression:

$$W_{ss,j} = \frac{Q_j}{EER_{ss}} \tag{7.4}$$

and

$$W_{ss} = \sum_j W_{ss,j} \tag{7.5}$$

It was noted, however, that EER_{ss} varied not only with T_j but with fractional on-time, Γ_i. This method results in estimates of the steady-state EER that were less than the cyclic EER for a significant number of cycles. The above mentioned variations were due in part to variation on the return air and return dew point temperature.

An alternative method for determining the steady-state seasonal performance was therefore used, incorporating the results of the previous section. It was noted that the part load performance factor, PLF_{ij}, and cooling load factor, CLF_{ij}, obtained from the scan data are a strong function of the fractional on-time, Γ_i (i denotes the fractional on-time bin) but insensitive to the outdoor temperature, T_j. It is assumed that PLF_{ij} and CLF_{ij} obtained from the scan data for each i, j bin are representative of all the cycles in that bin. From the analyses given in the Appendix, the seasonal part load performance factor is determined from the following expression:

$$PLF_{seas} = \sum_i PLF_i \quad \frac{W_{cyc,i}}{W} \tag{7.6}$$

Where $W_{cyc,i}$ = the energy used in a given fractional on-time bin, i.

In some instances scan data was totally lacking or insufficient to determine PLF_i for a given fractional on-time bin. In addition, the fractional on-time in each fractional on-time bin determined from the scan data varied slightly from the total (cycle) data for that bin.

In order to account for the above deficiencies in the data, the $\overline{PLF_i}$ were therefore determined by the following method. From the scan data, CLF was

plotted against fractional on-time, Γ_i, and a smooth curve was drawn. An example of the plot is given in figure 6.6. The fractional on-time determined from all the data was then determined for each i-bin and, using graphs similar to the one illustrated in figure 6.6, a CLF_i characteristic of that bin was read off it. The PLF_i were then determined from the performance curves given in figure 6.8, Section 6.3.3.

7.1 Seasonal Degradation Coefficient

The seasonal degradation coefficient is defined by the following expression:

$$C_{D_{seas}} = \frac{1 - PLF_{seas}}{1 - CLF(PLF_{seas})} \tag{7.7}$$

where the quantity $CLF(PLF_{seas})$ is the cooling load factor obtained from the part load performance curves of figure 6.8 at $PLF = PLF_{seas}$.

A 'seasonal cooling load factor', CLF_{seas}, may be defined as:

$$CLF_{seas} = \frac{Q}{\sum_i Q_{ss,i}} \tag{7.8}$$

where

$$\sum_i Q_{ss,i} = \sum_i \frac{Q_{cyc,i}}{CLF,i} \tag{7.9}$$

The quantity $Q_{ss,i}$ is the sum of the steady-state cooling over all cycles for a given i-bin. The steady-state cooling is that which would have occurred if

the unit operated steadily for the entire cycle time, τ, and at the same ambient condition existing during t_{on}.

It should be noted that in general CLF_{seas} and $CLF(PLF_{seas})$ are not equivalent. The former quantity is obtained by weighting with the fractional amount of cooling done whereas the latter value is dependent on the unit part load performance curve, weighted with the fractional amount of energy input.

The difference between CLF_{seas} as given by equation (7.8) and $CLF(PLF_{seas})$ is more clearly seen by assuming a linear relationship for the part load performance curve:

$$PLF = 1 - C_D(1 - CLF) \tag{7.10}$$

Applying equation (7.6) to equation (7.10) results in the following expression:

$$PLF_{seas} = 1 - C_D\left(1 - \sum_i CLF_i\left(\frac{W_i}{W}\right)\right) \tag{7.11}$$

The value of $CLF(PLF_{seas})$ is obtained by substituting the expression for PLF_{seas}, given by equation (7.11) into equation (7.10), which yields:

$$CLF(PLF_{seas}) = \sum_i CLF_i\left(\frac{W_i}{W}\right) \tag{7.12}$$

By comparing $CLF(PLF_{seas})$ as given by equation (7.12) and CLF_{seas} as defined through equations (7.8) and (7.9), it is evident that the two expressions are not equivalent.

Seasonal performance results of the three units are presented in Table 7.1. As discussed in Section 6.3, the factor 'c' appearing in the Table is a correction factor for the estimate of the steady-state latent capacity, which strongly influences the estimate for PLF_{seas}. The correction time, c = 2 min assumes that condensate does not start to form until 2 minutes after the unit cycles on, whereas c = 0 minutes assumes the unit is creating condensate at a steady-state rate as soon as the unit cycles on.

Table 7.1 Seasonal Field Performance Results

	c = 0			c = 2			c = 3			c = 4		
	$CLF(PLF_{seas})$	PLF_{seas}	C_D	$CLF(PLF_{seas})$	PLF_{seas}	C_D	$CLF(PLF_{seas})$	PLF_{seas}	C_D	$CLF(PLF_{seas})$	PLF_{seas}	C_D
Unit 1	.334	.940	.09	.330	.908	.14	.321	.889	.16	.312	.865	.20
Unit 2	.523	.943	.12	.515	.927	.15	.517	.917	.17	.514	.903	.20
Unit 3	.390	.918	.14	.380	.889	.18	.372	.880	.19	.367	.864	.22

where PLF_{seas} calculated from $\sum_i W_{ss,i} = \sum_i \overline{PLF}_i \, W_{cyc,i}$

C = 0 min = assumes $\frac{\dot{Q}^{\ell}_{cyc}}{\dot{Q}^{\tau}_{cyc}} = \frac{\dot{Q}^{\ell}_{ss}}{\dot{Q}^{\tau}_{ss}}$ = i.e., no latent correction

C = 2, 3, 4 min = correction for delay time for condensate to form during cyclic operation; increases s.s estimate for $\dot{Q}^{\ell}_{ss}$

CLF(PLF) calculated from field performance curves: $PLF = 1 - e^{-bx^c}$

8. COMPARISON OF LABORATORY AND SEASONAL FIELD PERFORMANCE RESULTS

The extensive data obtained from the field study were used to determine how well the present procedures [1,3] for determining the seasonal cooling performance of central air conditioners and heat pumps agree with actual field data. To this end, laboratory tests were conducted with an identical model as field unit number 3.

The following tests were conducted in the laboratory (as called for in the Test Procedures (1)).

	Indoor Dry-Bulb-Wet Bulb, °F	Outdoor Dry-Bulb Temperature, °F	Cycling Rate
Test A	80/67	95	steady-state
Test B	80/67	82	steady-state
Test C	80/dry-coil	82	steady-state
Test D	80/dry-coil	82	6 min-on, 24 min-off (Γ = .2)

Tests C and D are used to determine the cycling degradation coefficient, C_D, as follows:

$$PLF = \frac{EER(\text{Test D})}{EER(\text{Test C})} \tag{8.1}$$

$$CLF = \frac{\dot{Q}_{cyc}(\text{Test D})}{\dot{Q}_{ss}(\text{Test C})} \times \left(\frac{6}{(6 + 24)}\right) \tag{8.2}$$

$$C_D = \frac{1 - PLF}{1 - CLF} \qquad (8.3)$$

Because of the differences in cycling rates as required in the test procedures and the actual rate encountered in the field, Test D was also conducted at the typical field cycling rate for unit 3. The cycling rate was found to be closely approximated by the following relationship:

$$N = 6.55\,\Gamma\,(1 - \Gamma) \qquad (8.4)$$

(cycles per hour)

The laboratory unit was charged with refrigerant R22 at the same outdoor temperature and supply air quantity that occurred for a typical scan (detailed data) cycle of the field unit. Refrigerant charge was added or subtracted until the temperature difference across the coil agreed with the temperature difference that occurred for that cycle. Latent capacity was also checked to ensure agreement with the field performance for that 'typical' cycle. The ambient conditions of the selected cycle were:

IDB = 76°F	where	IDB	Indoor dry bulb temp.
IDP = 60.6°F		IDP	Indoor dew point temp.
ODB = 81°F		ODB	Outdoor dry bulb temp.
CFM = 1182 (1148 used in the laboratory tests)		CFM	Cubic feet per minute

A comparison of the steady-state capacity and power of the laboratory-tested unit and the field unit at an outdoor temperature of 82°F is given below:

	(Btu/h) $\dot{Q}_{ss}(82)$	(watts) $\dot{W}_{ss}(84)$	$EER_{ss}(82)$	
Laboratory Unit	32,030	4021	7.97	
Field Unit	30,144	4143	7.3	c = 2 min
	(28,550)	4143	(6.9)	(c = 0 min)

Field data at an outdoor temperature of 95°F is not reported since no direct scan data were available.

The capacity and energy efficiency ratio results for the field unit were obtained through an estimate of the steady-state latent capacity. The results for c = 0 were obtained by assuming that the ratio of steady-state latent to steady-state sensible capacities are the same as in cyclic operation. As can be seen, there is a significant difference in results. Laboratory investigations, however, have indicated that in cyclic operation, condensate is not generated until 2 to 4 minutes after the unit cycles on. Hence, for short on-times the ratio of steady-state latent to steady-state sensible capacity is greater than the cyclic ratio. Using this new estimate, the results are reported in the above table for c = 2 minutes. Other factors which contribute to the variations in results are the lower entering dry-bulb and wet-bulb temperatures (approximately 76°F and 66°F, respectively) for the field unit than the laboratory test conditions (80°F/67°F).

A comparison of the field and laboratory cyclic performance results can be made with the aid of Table 8.1 and figure 8.1. As discussed earlier, the constants c = 0, 2, 4 minutes appearing in the field performance results are

Table 8.1 Comparison of Laboratory and Field Cyclic Performance

	Fractional On-Time Γ, Thermostat Setting, N_{max} (cycle/hr)	On-Off Times (Min) t_{on}/t_{off}	C_D
Laboratory Results	$N_{max} = 3$		
	$\Gamma = .2$	6/24	.36
	$\Gamma = .5$	10/10	.31
	$N_{max} = 1.64$		
	$\Gamma = .2$	11.5/46	.21
	$\Gamma = .5$	11/18	.23
Field Results (Seasonal Values)	c = 0 min c = 2 min ($N_{max} = 1.64$) c = 4 min		.14 .18 .22

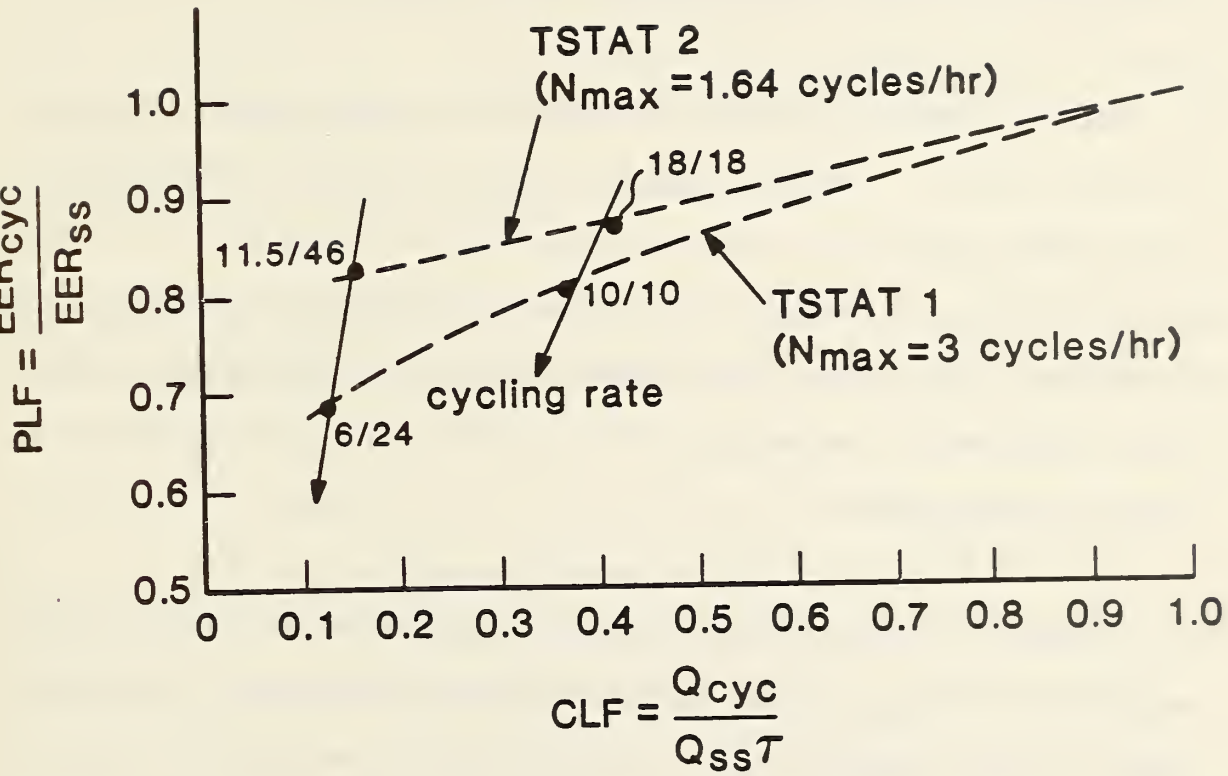

Figure 8.1. Laboratory cyclic performance results.

estimates of the time required after the unit cycles on for condensate to form on the coil, and as a result, affect the estimate for total steady-state capacity. Based on previous laboratory tests, a value of c = 2 is judged to be a reasonable (conservative) estimate. This value should therefore be used in comparing the field results with laboratory results.

The laboratory results presented in Table 8.1 have been divided into two operating regions: the first (N_{max} = 3 cph) corresponds to a thermostat setting which results in a maximum cycling rate of 3 cycles/hr at Γ = 0.5 and the second (N_{max} = 1.64 cph) is the thermostat setting approximating the field measurements. The present test procedure calls for a thermostat setting of N_{max} = 3 cph and Γ = 0.2 which results in on-off times of 6 minutes and 24 minutes, respectively.

The laboratory results indicate a relatively high value of the degradation coefficient for N_{max} = 3 cph, Γ = 0.2 (6 min on, 24 min off). A slightly lower value was obtained for Γ = 0.5 (10 min on, 10 min off) but still high compared to field performance results.

Much better agreement in the degradation coefficient is shown for a thermostat setting equal to 1.64 cph. A slightly anomolous trend is observed in the laboratory results for Γ = 0.2 (C_D = .21) and Γ = 0.5 (C_D = .23). This is most probably due to the rounding of the on-off times for convenience in testing.

9. CONCLUSIONS

Field data were collected and the cooling performance of three heat pump units evaluated. Two major types of data were collected and used to evaluate the cyclic performance parameters and seasonal performance. The first type consisted of scan data collected at various intervals during the on portion of a cycle. The second type consisted of cycle data in which data was averaged or summed, as appropriate, for an entire on-off cycle. Cycle data was collected for every cycle throughout the test period.

Scan data for every tenth on-off cycle was collected and used to evaluate the cyclic performance parameters. The results confirmed laboratory findings that the cooling load and part load factors are independent of the outdoor temperature and dependent only on the cycling rate and fractional on-time. From the scan data, part load performance curves were generated and in conjunction with the cycle data, seasonal part load factors and cyclic degradation coefficients determined. The methodology utilized performance data from the units and therefore did not require incorporating a building cooling load assumption.

Field thermostat data were collected and a semi-empirical model was developed. The model was found to be in excellent agreement with the data. Peak cycling rates, occurring at fractional on-times of 0.5 were found to range from approximately 1.6 cph to 2.3 cph. The predicted cycling rate at a fractional on-time of 0.5 resulting from cycling at the rate called for in the standard test and rating procedures [1,3] is 3 cph, higher than observed for the three field units. It is believed that factory settings for the cooling anticipator

and commonly used mercury bulb electromechanical thermostats result in peak cycling rates ranging from approximately 2 cph to an upper limit of 3 cph [5].

Cooling performance tests were conducted in the laboratory on an identical model heat pump as was tested in the field. At an outdoor tempeature of 82°F, the steady-state capacity, power, and EER of the laboratory unit were within 6 percent, 3 percent, and 9 percent, respectively of the field unit. The above differences were attributed to a) lower average return-air dry-bulb (76°F) and wet-bulb (66°F) temperatures for the field unit as compared to laboratory conditions (80°F dry-bulb, 67°F wet-bulb temperature), b) approximation used in determining the steady-state latent (and hence) total capacity of the field unit, and c) manufacturing tolerances listed in order of importance.

Cycling tests were also conducted in the laboratory in accordance with the standard test and rating procedures [1,3] in order to compare and evaluate the cyclic degradation coefficient, C_D, with field results. Cycling the unit at the standard rate of 6 minutes-on, 24 minutes-off resulted in a value of C_D = 0.36. The result is significantly different than the field result, C_D = 0.18. The laboratory unit was then cycled at the same avarage rate as the field unit corresponding to a fractional on-time, Γ, equal to 0.2 (11.5 minutes-on, 46 minutes-off). The cyclic degradation coefficient resulting from this rate was found to be in much better agreement (C_D = .21) with the field results. The remaining disparity between laboratory and field results are attributed to a) differences in the amount of refrigerant charge in the two units, and b) approximations used in the field results for evaluating the steady-state latent capacity.

The laboratory test procedures [1,3] used to determine the cyclic degradation coefficient from dry coil tests appear to accurately reflect the degradation coefficient found in actual practice, as long as comparable thermostat charcteristics (reflected by the peak cycling rate N_{max} at 0.5 fractional on-time) are employed. It is apparent that the standard laboratory cycling rate is too high and that a somewhat lower rate, ranging between $N_{max} = 2$ and $N_{max} = 3$ should be employed.

10. REFERENCES

1. Kelly, G.E., and Parken, W.H., "Method of Testing, Rating and Estimating the Seasonal Performance of Central Air-Conditioners and Heat Pumps Operating in the Cooling Mode," National Bureau of Standards, NBSIR 77-1271 (April 1978).

2. Parken, W.H., Kelly, G.E., and Didion, D.A., "Method of Testing, Rating and Estimating the Heating Seasonal Performance of Heat Pumps," National Bureau of Standards, NBSIR 80-2002 (April 1980).

3. Federal Register, Part III, Department of Energy, Office of Conservation and Solar Energy, Test Procedures for Central Air Conditioners, Including Heat Pumps, Thursday, December 27, 1979.

4. Hurley, C.W., Kelly, G.E., and Kopetka, P.A., "Using Microcomputers to Monitor the Field Performance of Residential Heat Pumps," National Bureau of Standards, NBSIR 81-2285 (June 1981).

5. Private communications with Lorne Nelson of Honeywell.

APPENDIX

A.1 THERMOSTAT MODEL

The development of the thermostat model rests on several simplifying assumptions so that only a brief discussion is justified.

The building cooling load, BL, is assumed to be met over the cycle time period, τ, by the cooling done (by the unit) during the on time, t_{on}. This is expressed as:

$$\frac{t_{on}}{\tau} = \frac{BL}{\dot{Q}_{cyc}} \qquad A.1(1)$$

where the fractional on time, t_{on}/τ is dominated by variations in BL. The variation in unit cyclic capacity, $\dot{Q}_{cyc}$ due to outdoor temperature and cycling rate is small in comparison to changes in BL so that the former is considered constant. Equation A.1(1) is therefore written as:

$$\frac{t_{on}}{\tau} = K_1 BL \qquad A.1(2)$$

A thermostat has a built-in temperature differential, $T^* - T_{crit}$ which is normally on the order of 3°F. When the indoor air temperature reaches a value T^* above the set point, T_{set}, the thermostat calls for cooling. The indoor air temperature decreases while the unit is on, to a value, T_{crit} below T_{set} before turning off. The following figure illustrates the indoor air temperature variation as the cooling unit goes through a complete on-off cycle.

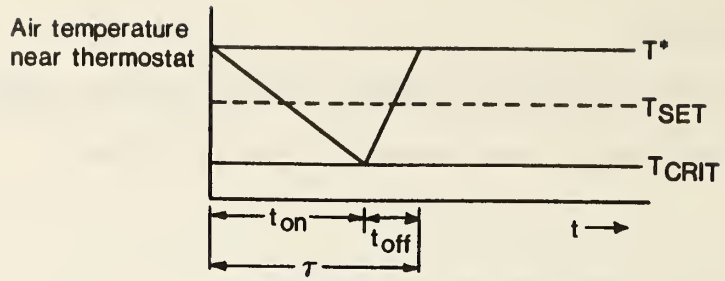

A second simplifying assumption made is that the building cooling load is proportional to the rate of increase in the indoor air temperature when the unit is off. This is expressed as:

$$BL = K_2 \frac{T^* - T_{crit}}{t_{off}} \qquad A.1(3)$$

The quantity $K(T^* - T_{crit})$ incorporates heat transfer and storage effects of the building interior surfaces to the indoor air as well as the thermostat differential. The above quantity can be adjusted to any desired value by means of a thermostat anticipator circuit. The anticipator heats the air near the bimetallic element during the unit off period. The following figure illustrates ideally how the anticipator regulates the length of the unit off-time.

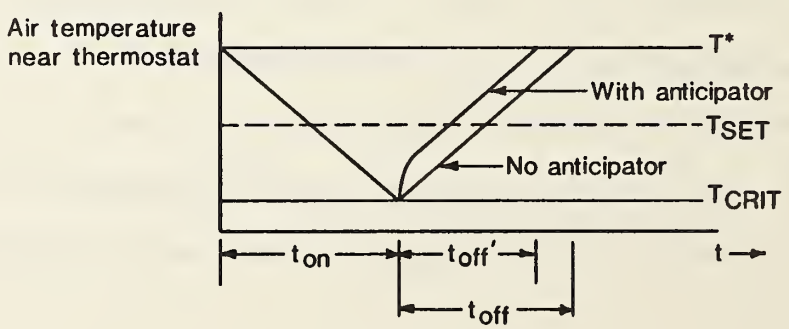

The above discussed quantity, $K_2(T^* - T_{crit})$ is herein considered constant with respect to changing building loads and fractional on-times. Equation A.1(3) is then written as:

$$BL = \frac{K_3}{t_{off}} \qquad A.1(4)$$

Combining the following definitions:

$$\tau = t_{on} + t_{off} \qquad A.1(5)$$

$$N = \frac{1}{\tau} \qquad A.1(6)$$

with equations A.1(2) and A.1(4) the following expression is obtained

$$N = K \frac{t_{on}}{\tau} (1 - \frac{t_{on}}{\tau}) \qquad A.1(7)$$

Recognizing that the maximum cycling rate, N_{max}, occurrs as $t_{on}/\tau = .5$, the above expression is written as:

$$N = 4 N_{max} \Gamma (1 - \Gamma) \qquad A.1(8)$$

where N_{max} is the cycling rate at 50 percent on time and Γ is the fractional on-time (t_{on}/τ).

A.2 DEVELOPMENT OF METHOD TO IMPROVE THE ESTIMATE FOR STEADY-STATE CAPACITY, COOLING LOAD FACTOR AND PART LOAD FACTOR

Observations made during laboratory tests indicate that condensate starts to form from 2 to 4 minutes after unit start-up.

In the field, condensate was measured only over a complete cycle. In the initial calculations of the steady-state latent capacity the following relationship was assumed:

$$\frac{\dot{Q}^{\ell}_{cyc}}{\dot{Q}^{T}_{cyc}} = \frac{\dot{Q}^{\ell}_{ss}}{\dot{Q}^{T}_{ss}} \text{ or equivalently } \frac{\dot{Q}^{s}_{cyc}}{\dot{Q}^{T}_{cyc}} = \frac{\dot{Q}^{s}_{ss}}{\dot{Q}^{T}_{ss}} \qquad \text{A.2(1)}$$

where the superscripts ℓ, s, T denote latent, sensible and total, respectively. For small on-times it is evident that equation A.2(1) underestimates the steady-state latent capacity.

To improve the estimate of the latent steady-state capacity the following relationship was assumed:

$$\frac{\dot{Q}^{\ell}_{ss}}{\dot{Q}^{s}_{ss}} = \frac{Q^{\ell}_{cyc}}{(t_{on} - c)} \Big/ \left(\frac{Q^{s}_{cyc}}{t_{on}}\right) \qquad \text{A.2(2)}$$

where c denotes the delay time (ranging from two to four minutes) before condensate starts to form after the unit has cycled on.

Using the relationship:

$$\frac{Q^{\ell}_{cyc}}{Q^{s}_{cyc}} = \frac{Q^{T}_{cyc}}{Q^{s}_{cyc}} - 1,$$

and combining with equations A.2(1) and A.2(2), the following equation applies:

$$\frac{\dot{Q}^{\ell}_{ss}}{\dot{Q}^{s}_{ss}} = \left[\frac{Q^{T}_{cyc}}{Q^{s}_{cyc}} - 1\right]\left[\frac{1}{1 - c/t_{on}}\right] \qquad \text{A.2(3)}$$

Equation A.2(3) is further rearranged to the form:

$$\frac{\dot{Q}^{\ell}_{ss}}{\dot{Q}^{s}_{ss}} = \left[\frac{Q^{T}_{cyc}}{Q^{s}_{cyc}} - 1\right]\left[\frac{1}{1 + D}\right] \qquad \text{A.2(4a)}$$

where

$$D = -c/t_{on} \qquad \text{A.2(4b)}$$

The steady-state total capacity is expanded to the form:

$$\dot{Q}^{T}_{ss} = \dot{Q}^{s}_{ss}\left[1 + \frac{\dot{Q}_{ss}}{\dot{Q}^{s}_{ss}}\right] \qquad \text{A.2(5)}$$

Combining equation A.2(4a) and A.2(5) results in the following expression for the total steady-state capacity:

$$\dot{Q}^{T}_{ss} = \dot{Q}^{s}_{ss}\left[1 + \left(\frac{Q^{T}_{cyc}}{Q^{s}_{cyc}} - 1\right)\left(\frac{1}{1 + D}\right)\right] \qquad \text{A.2(6)}$$

The above expression is rearranged to:

$$\dot{Q}^{T}_{ss} = \frac{\tilde{Q}^{T}_{ss} + D\ \dot{Q}^{s}_{ss}}{1 + D} \qquad \text{A.2(7)}$$

where $\tilde{Q}^{T}_{ss}$ denotes the 'uncorrected' total steady-state capacity as determined from equation A.2(1). In the subsequent derivations, all variables written with a ~ (telda) denote quantities uncorrectd for the improved estimate in the latent steady-state capacity.

The steady-state energy efficiency ratio, EER_{ss} can be evaluated in terms of the uncorrected estimate $\tilde{EER}_{ss}$ using equation A.2(7) as:

$$EER_{ss} = \frac{\dot{Q}^{T}_{ss}}{W_{ss}} = \frac{\tilde{EER}_{ss} + \frac{D\ Q_{ss}}{W_{ss}}}{1 + D} \qquad \text{A.2(8)}$$

The part-load factor, PLF is expressed in terms of the uncorrected $\tilde{PLF}$ and the uncorrected ratio of steady-state sensible and steady-state total capacity using equation A.2(8)

$$\frac{1}{PLF} = \left[\frac{EER_{ss}}{EER_{cyc}}\right] = \left[\frac{\tilde{EER}_{ss}}{EER_{cyc}} + \frac{1}{EER_{cyc}}\left(\frac{D\ \dot{Q}^{s}_{ss}}{W_{ss}}\right)\right] \Big/ 1 + D \qquad \text{A.2(9a)}$$

Equation A.2(9a) can be simplified to the following expression:

$$\frac{1}{PLF} = \frac{1}{\tilde{PLF}}\left[1 + \frac{D\ \dot{Q}^{s}_{ss}}{\dot{Q}^{s}_{ss}}\right] \qquad \text{A.2(9b)}$$

where as noted is equation A.2(1):

$$\frac{\dot{Q}^{s}_{ss}}{\tilde{\dot{Q}}^{T}_{ss}} = \frac{\dot{Q}^{s}_{cyc}}{\dot{Q}^{T}_{cyc}}$$

The cooling load factor, CLF, can be evaluated from the uncorrected estimate, $\tilde{CLF}$ by using the following relationship:

$$\frac{1}{CLF} = \frac{\tau}{t_{on}}\frac{\dot{Q}^{T}_{ss}}{\dot{Q}^{T}_{cyc}} = \frac{\tau}{t_{on}}\left(\frac{\tilde{\dot{Q}}^{T}_{ss} + D\ \dot{Q}^{s}_{ss}}{(1 + D)Q^{T}_{cyc}}\right) \qquad \text{A.2(9)}$$

Using the above relationship equation A.2(9) can be reduced to the following expression:

$$\frac{1}{CLF} = \frac{1}{\tilde{CLF}}\left(\frac{1 + D\ \dfrac{\dot{Q}^{s}_{ss}}{\tilde{\dot{Q}}^{T}_{ss}}}{1 + D}\right)$$

A.3 DETERMINATION OF SEASONAL PART LOAD FACTOR

The seasonal part load performance, PLF_{seas}, is defined by the following expression:

$$PLF_{seas} = \frac{SEER}{SEER_{ss}} \qquad A.3(1a)$$

where $SEER = Q/W$ A.3(1b)

$$SEER_{ss} = Q/W_{ss} \qquad A.3(1c)$$

Q = total measured seasonal cooling

W = total measured seasonal energy used

The term W_{ss} is the seasonal energy usage that would have occurred if the unit operated with no part load losses. This term is evaluated by first considering a single cycle, k, in temperature bin j with fractional on time, i. The steady-state (ideal) energy input for a single cycle, $W_{ss,ijk}$ may be expressed as:

$$W_{ss,ijk} = \dot{W}_{ss,ij}\ t'_{on,ijk} \qquad A.3(2)$$

where $t'_{on,ijk}$ = the 'ideal' time the unit would have been on to satisfy the cooling load if the unit had no part load losses.

$\dot{W}_{ss,ij}$ = the steady-state power input of the unit for temperature bin j and fractional on-time, i

The 'ideal' on-time, $t'_{on,ijk}$ is determined by the cooling load balance equations:

$$BL\ \tau_{ijk} = \dot{Q}_{cyc,ij}\ t_{on,ijk} \qquad A.3(3)$$

$$BL\ \tau'_{ijk} = \dot{Q}_{ss,ij}\ t'_{on,ijk} \qquad A.3(4)$$

where BL = building cooling load

τ = total time for one complete cycle.

A one-to-one correspondence between 'ideal' and actual cycle times can be maintained if in the ideal case the anticipator is readjusted. This equivalence is stated here for convenience:

$$\tau'_{ijk} = \tau_{ijk} \qquad A.3(5)$$

Thus in the 'ideal' case and actual case, the building load is met over the same time periods.

Using equations A.3(3), A.3(4) and A.3(5), the 'ideal' on time is written as:

$$t'_{on,ijk} = \frac{\dot{Q}_{cyc,ij}}{\dot{Q}_{ss,ij}}\ t_{on,ijk} \qquad A.3(6)$$

Using the expression with equation A.3(2), gives:

$$W_{ss,ijk} = \dot{W}_{ss,ij}\ \frac{\dot{Q}_{cyc,ij}}{\dot{Q}_{ss,ij}}\ t_{on,ijk} \qquad A.3(7)$$

the above expression is expanded as follows:

$$W_{ss,ijk} = \frac{\dot{W}_{ss,ij}}{\dot{W}_{cyc,ij}} \frac{\dot{Q}_{cyc,ij}}{\dot{Q}_{ss,ij}} \frac{\dot{Q}_{ss,ij}}{\dot{Q}_{cyc,ij}} \dot{W}_{cyc,ij} \left[\frac{\dot{Q}_{cyc,ij}}{\dot{Q}_{ss,ij}} t_{on,ijk}\right] \qquad A.3(8)$$

Equation A.3(8) reduces to:

$$W_{ss,ijk} = PLF_{ij} W_{cyc,ijk} \qquad A.3(9)$$

where

$$PLF_{ij} = \frac{EER_{cyc,ij}}{EER_{ss,ij}} \qquad A.3(10)$$

$$W_{cyc,ijk} = \dot{W}_{cyc,ijk} t_{on,ijk} \qquad A.3(11)$$

The seasonal energy usage that would have occurred if the unit had no part-load losses is the sum over all cycles, m_{ij}, in each, i, j bin. This is written as:

$$W_{ss} = \sum_i \sum_j \sum_k^{m_{ij}} W_{ss,ijk} \qquad A.3(12)$$

$$W_{ss} = \sum_i \sum_j \sum_k^{m_{ij}} PLF_{ij} W_{cyc,ijk}$$

As discussed in the text, the part load factor, PLF_{ij}, is relatively insensitive to outdoor temperature. A mean value is determined from the data

for all cycles for a given fractional on-time bin, i. The above expression therefore reduces to

$$W_{ss} = \sum_i PLF_i \, W_{cyc,i} \qquad \text{A.3(13)}$$

where $$W_{cyc,i} = \sum_j W_{cyc,ij} \qquad \text{A.3(14)}$$

Combining equations A.3(13) with equation A.3(1a), A.3(1b) and A.3(1c) results in the following expression:

$$PLF_{seas} = \frac{1}{W} \sum_i PLF_i \, W_{cyc,i} \qquad \text{A.3(15)}$$

NBS-114A (REV. 2-8C)

U.S. DEPT. OF COMM. BIBLIOGRAPHIC DATA SHEET (See instructions)	1. PUBLICATION OR REPORT NO. NBSIR 85-3107	2. Performing Organ. Report No.	3. Publication Date March 1985

4. TITLE AND SUBTITLE

Field Performance of Three Residential Heat Pumps in the Cooling Mode

5. AUTHOR(S)

Walter Parken, David Didion, Lih Chern and Paul Wojciechowski

6. PERFORMING ORGANIZATION (If joint or other than NBS, see instructions)

NATIONAL BUREAU OF STANDARDS
DEPARTMENT OF COMMERCE
WASHINGTON, D.C. 20234

7. Contract/Grant No.

8. Type of Report & Period Covered

9. SPONSORING ORGANIZATION NAME AND COMPLETE ADDRESS (Street, City, State, ZIP)

U.S. Department of Energy
1000 Independence Avenue, S.W.
Washington, D.C. 20585

10. SUPPLEMENTARY NOTES

[ ] Document describes a computer program; SF-185, FIPS Software Summary, is attached.

11. ABSTRACT (A 200-word or less factual summary of most significant information. If document includes a significant bibliography or literature survey, mention it here)

Field data was acquired for three residential heat pumps and the part load performance factor and seasonal cooling energy efficiency ratio were evaluated. Laboratory tests were conducted on a unit identical to one of the field-tested heat pumps and performance results compared. Thermostat data was also acquired and a semi-empirical model developed.

The thermostat model was found to be in excellent agreement with the field data for all three field units and could be characterized by a peak cycling rate, N_{max}, occuring at a fractional on-time of 0.5. The value of N_{max} was found to range from 1.64 cycles per hour to 2.28 cycles per hour.

The laboratory test results indicated a higher cyclic degradation coefficient than found for the field unit when cycled at a rate of 6 minutes on, 24 minutes off (corresponding to N_{max} = 3 cycles per hour). However, when the laboratory unit was cycled at the same (lower) rates as found for the field unit (corresponding to N_{max} = 1.64 cycles per hour), the cyclic degradation coefficient and seasonal part load factors were in good agreement.

12. KEY WORDS (Six to twelve entries; alphabetical order; capitalize only proper names; and separate key words by semicolons)

central air-conditioning; cooling field performance; energy conservation; field data acquisition; heat pumps; thermostats

13. AVAILABILITY

[x] Unlimited
[ ] For Official Distribution. Do Not Release to NTIS
[ ] Order From Superintendent of Documents, U.S. Government Printing Office, Washington, D.C. 20402.
[x] Order From National Technical Information Service (NTIS), Springfield, VA. 22161

14. NO. OF PRINTED PAGES

86

15. Price

$11.50